Theory…..and experiment

Ultra-brief summary:

1) Atoms have a spin (S) and orbital (L) moment

2) Competition between $V_{e\text{-}e}$ and CF determine S and L:

- a) 3d metals — if $V_{e\text{-}e}$ > CF -> high spin; if $V_{e\text{-}e}$ < CF -> low spin
- b) rare earth — $V_{e\text{-}e}$ > CF -> high spin

3) SOC (ξLS) locks S to L

4) Competition between CF and SOC determine the MAE

- a) in 3d metals — CF > SOC
- b) rare earth — SOC > CF

Experimentally: how do we get information about all of this?

CF -> bond formation -> modified valence state (and also core level)

XPS *vs.* XAS

XAS

X-ray absorption spectroscopy

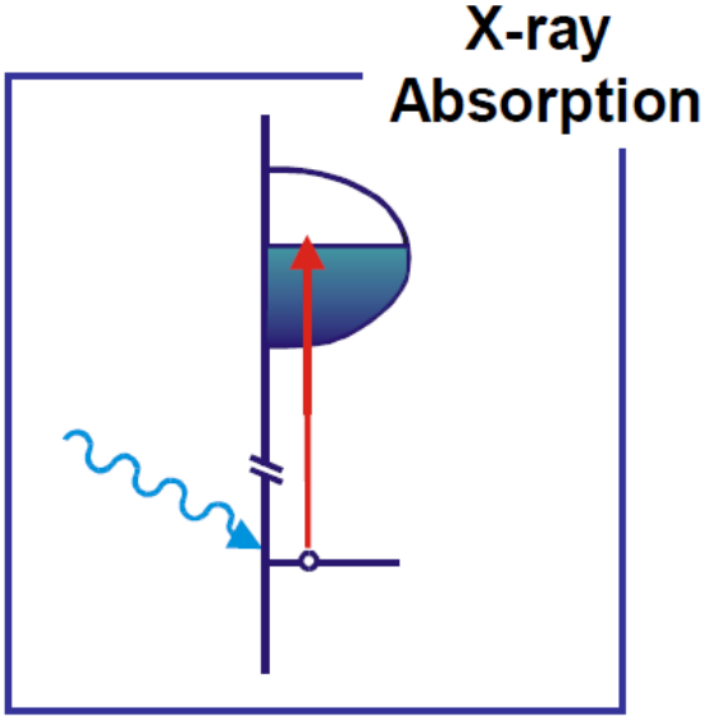

Access to modified core and valence states

XPS

X-ray photon spectroscopy

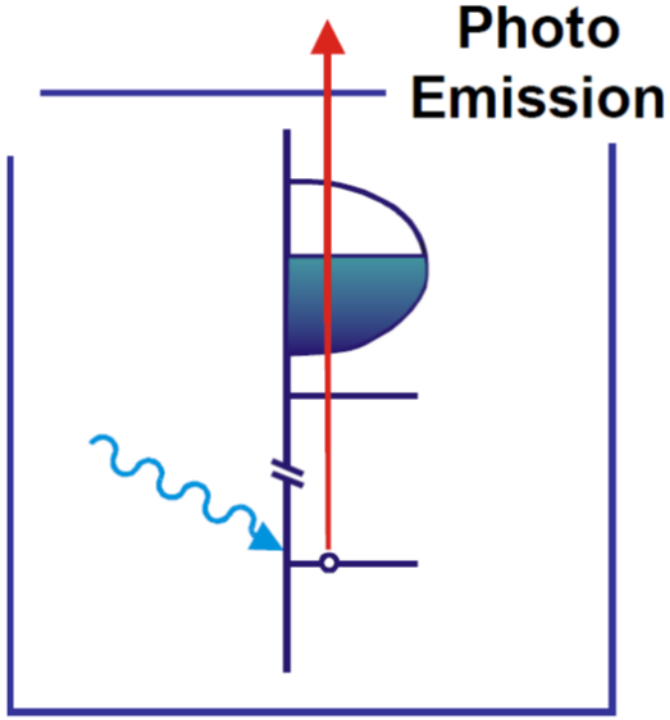

Access to modified core states

X-rays spectroscopy

$$H = H_{atom} + H_{crystal-field}$$

$$H_{atom} = \sum \frac{p_i^2}{2m} - \sum \frac{Ze^2}{r_i} + \sum \frac{e^2}{r_{ij}} + \sum \xi(r_i)\, l_i \bullet s_i; \quad H_{crystal-field} = -e\phi(r)$$

XAS

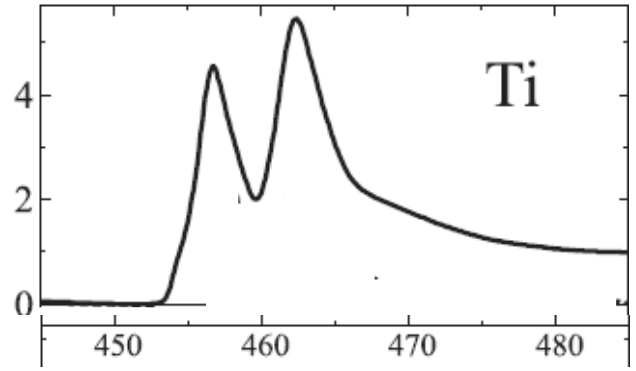

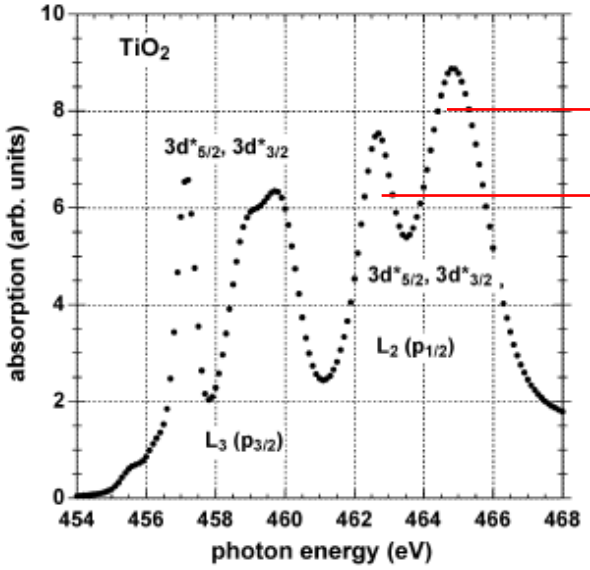

XPS

Spin-orbit coupling of the 2p core levels

Core level shift

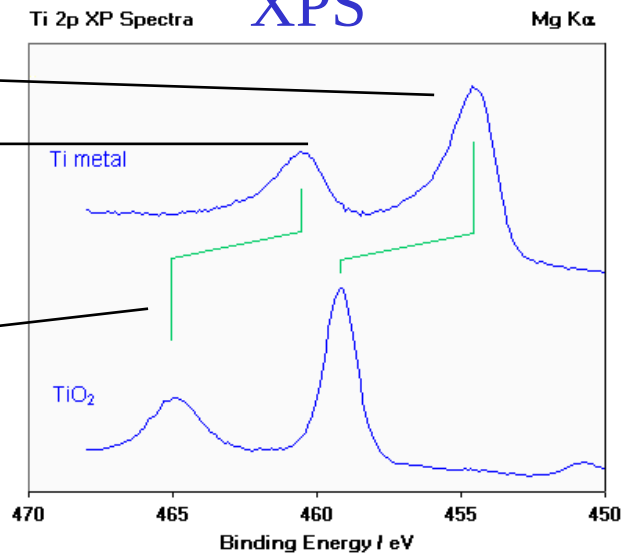

Crystal field and spin-orbit splitting of the 3d valence states

- The XAS spectrum is a convolution of the core levels and valence states
- 3d valence states are strongly affected by the hybridization with the oxygen atoms (Crystal field)

Valence band: 3d vs. 4f metals

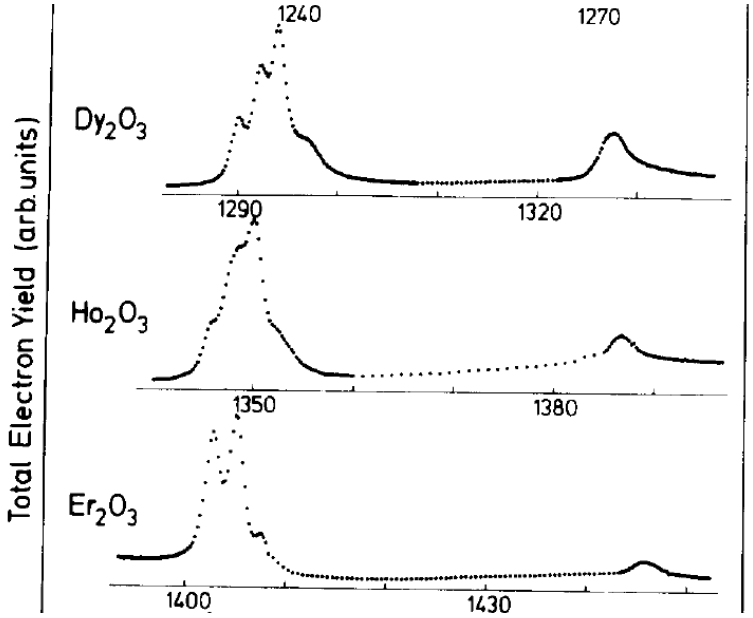

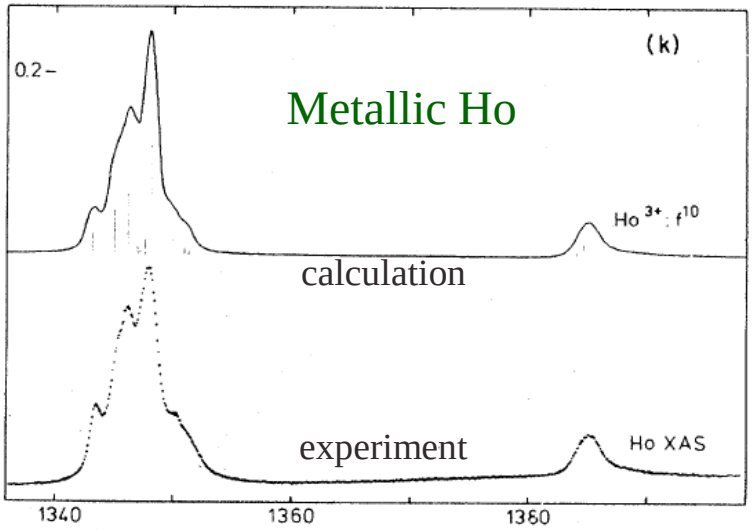

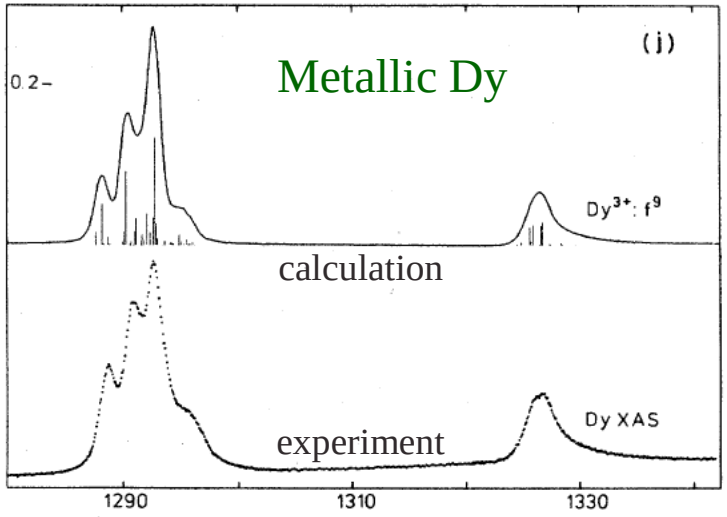

- The XAS spectrum of rare earth in a metal or in an oxide are very similar
- 4f valence states are strongly localized and only slightly affected by the hybridization with the oxygen atoms (Crystal field)

X-rays absorption and X-ray magnetic circular dichroism (XMCD)

Two step model:

1) spin-polarized photoelectrons are created by using circularly polarized x-rays
2) these polarized photoelectrons are used to analyze the spin-split valence density of states, thus the valence band acts as a spin-sensitive detector.

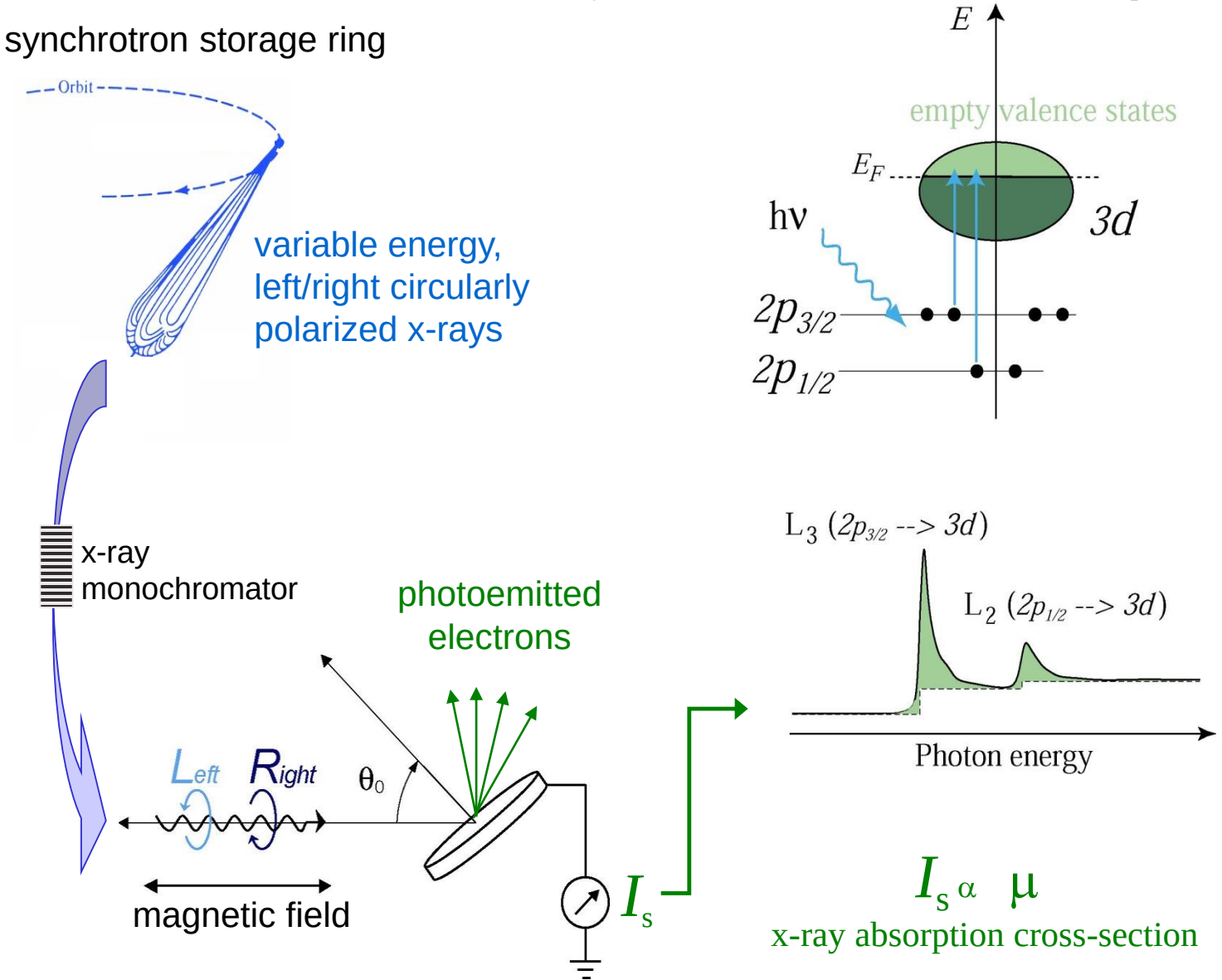

XMCD theory: basic idea

Photon-electron interaction: dipole approximation $H_{int}(0,t) \approx \underline{r}\cdot\underline{\varepsilon}_q\,[a_k \exp(-i\omega_k t) + c.c.]$

The dipole operator $P_q^1 = \underline{r}\cdot\underline{\varepsilon}_q$ can be written in terms of Racah's tensor operators (where $Y_{l,m}$ are the spherical harmonics)

$\underline{\varepsilon}_q$ is the polarization dependent electric vector

q = 0 -> linear polarization
q = +/- 1 -> circular polarization

$$P_{\pm1}^{(1)} = \mp\frac{1}{\sqrt{2}}(x \pm iy) = rC_{\pm1}^{(1)} = r\sqrt{\frac{4\pi}{3}}Y_{1,\pm1}$$

$$P_0^{(1)} = z = rC_0^{(1)} = r\sqrt{\frac{4\pi}{3}}Y_{1,0}$$

The photon absorption generates a transition from an initial core level to a final level close to the Fermi level (note that the spin is not affected)

$$|i\rangle = R_i(r)\,|c, m_c; s = \frac{1}{2}, m_s\rangle \longrightarrow |f\rangle = R_f(r)\,|l, m_l; s = \frac{1}{2}, m_s\rangle$$

$\langle l,m\|C_{\pm1}^{(1)}\|l-1,m\mp1\rangle = \sqrt{\frac{(l\pm m)(l\pm m-1)}{2(2l-1)(2l+1)}}$	$\langle l,m\|C_{\pm1}^{(1)}\|l+1,m\mp1\rangle = -\sqrt{\frac{(l\mp m+2)(l\mp m+1)}{2(2l+3)(2l+1)}}$
$= \sqrt{\frac{l(l-1)\pm(2l-1)m+m^2}{2(2l-1)(2l+1)}}$	$= -\sqrt{\frac{l(l+3)\mp(2l+1)m+m^2}{2(2l+3)(2l+1)}}$
$\langle l,m\|C_0^{(1)}\|l-1,m\rangle = \sqrt{\frac{l^2-m^2}{(2l-1)(2l+1)}}$	$\langle l,m\|C_0^{(1)}\|l+1,m\rangle = \sqrt{\frac{(l+1)^2-m^2}{(2l+3)(2l+1)}}$

Table 1.3: Electric dipole matrix elements $\langle l, m_l|C_q^{(1)}|c, m_c\rangle$ in the one electron model. The matrix elements are non-vanishing when $c = l-1$ (left column) or $c = l+1$ (right column), and when $m_c + q = m_l$. q denotes the state of polarization of the photons which mix the states $|l, m_l\rangle$ and $|c, m_c\rangle$.

Remember: things become easily complicate. For example, if spin-orbit interaction is not negligible the (L, m_L, S, m_S) is not the good basis and you have to use the (L, S, J, m_J) basis

X-rays absorption and X-ray magnetic circular dichroism (XMCD)

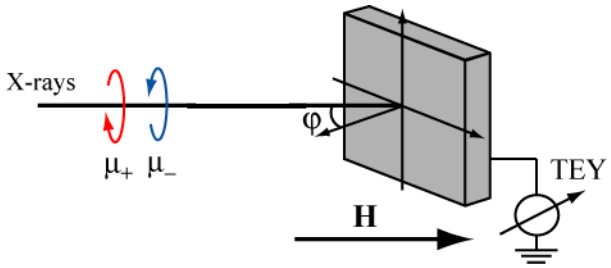

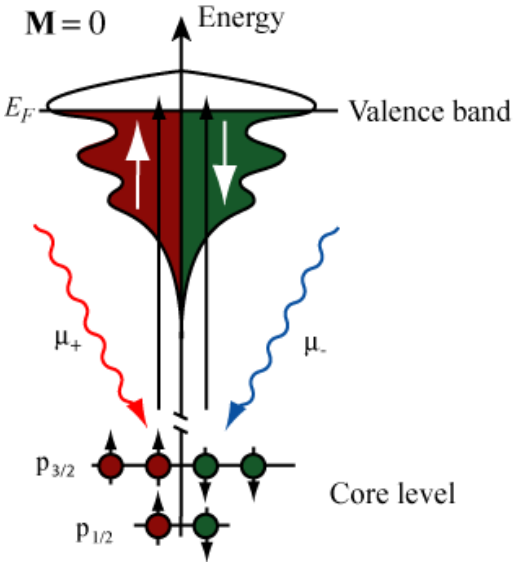

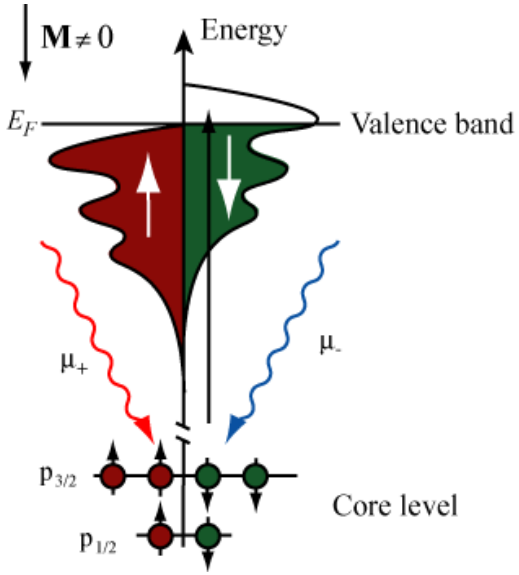

μ in dipole approximation

$$\mu \propto \left|\langle f|\varepsilon r|i\rangle\right|^2 \delta(\hbar\omega-(E_f-E_i))\rho(E_f)$$

Dipole selection rules

$\Delta l = \pm 1, \Delta s = 0$ 2p → 3d, 4s

$\Delta m_l = +1$ right circular

$\Delta m_l = -1$ left circular

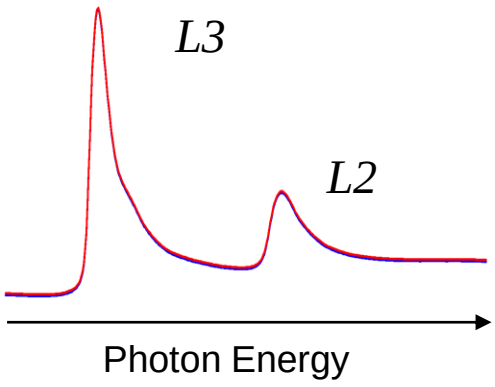

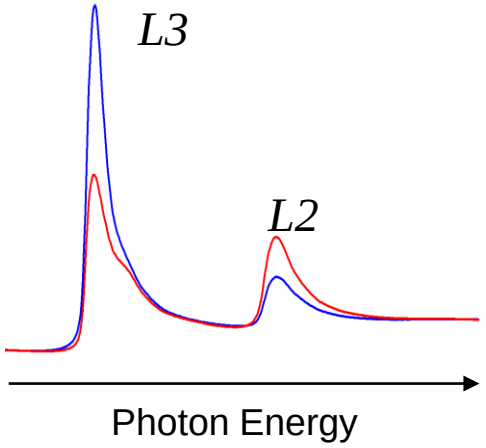

2p -> 4s transitions account for less than 5% of the total XAS intensity -> neglected

X-rays absorption and X-ray magnetic circular dichroism (XMCD)

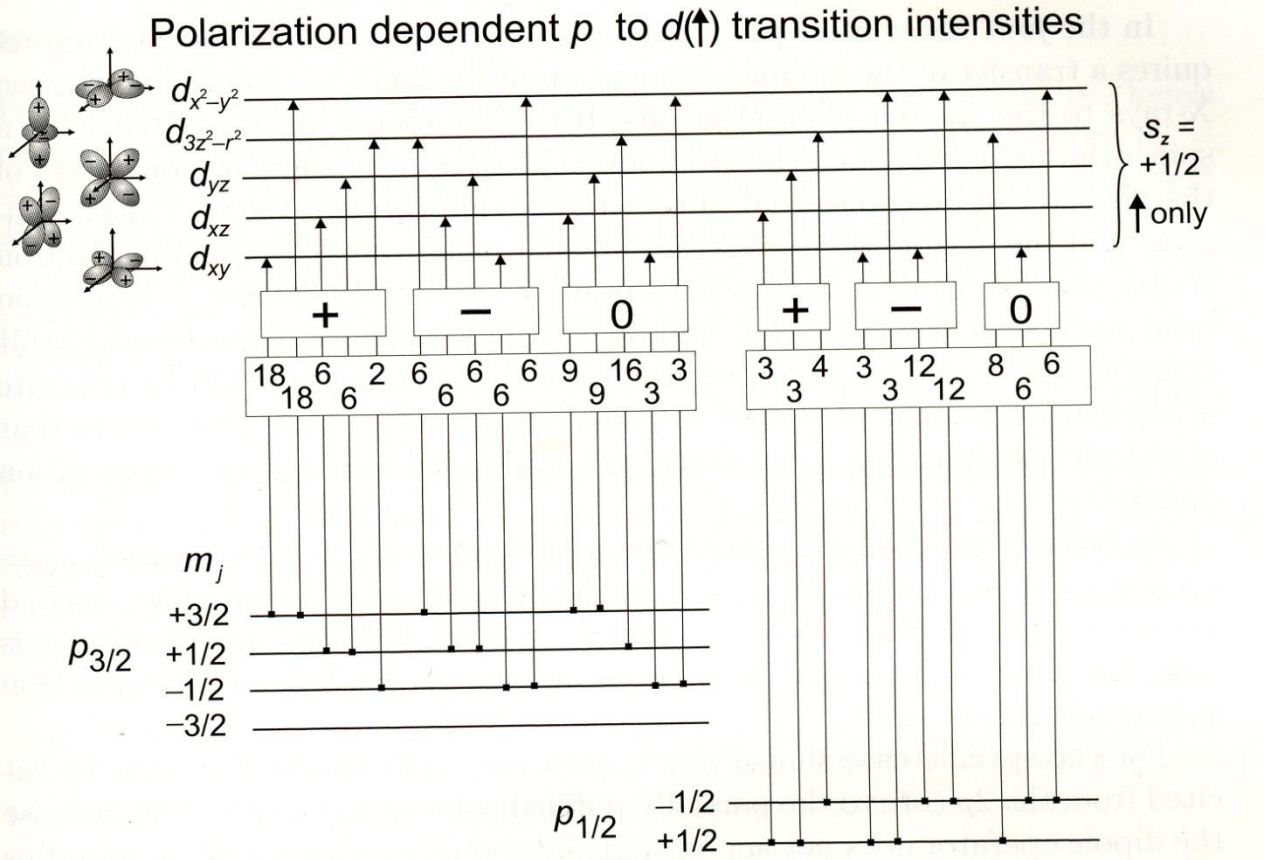

Fig. 9.14. Polarization dependent transition intensities in a one-electron model from spin–orbit and exchange split p core states $|j, m_j\rangle$ to *spin-up* ($m_s = +1/2$) d valence orbitals (Table A.2), assumed to be split by the exchange interaction. The listed intensities each need to be divided by 90 to get the proper absolute values in units of $\mathcal{AR}^2$. We have chosen the z-axis as the spin quantization axis and the transition intensities are for circular polarization with $\boldsymbol{k} \parallel z$ and angular momenta $q = +1$ (labeled +) and $q = -1$ (labeled −) and for linear polarization with $\boldsymbol{E} \parallel z$ (labeled $q = 0$). We have assumed a splitting of the p states by the exchange interaction, lifting the degeneracy in m_j. Note that this causes an opposite order of m_j states for $p_{3/2}$, $l + s$ and $p_{1/2}$, $l - s$ because of the opposite sign of s

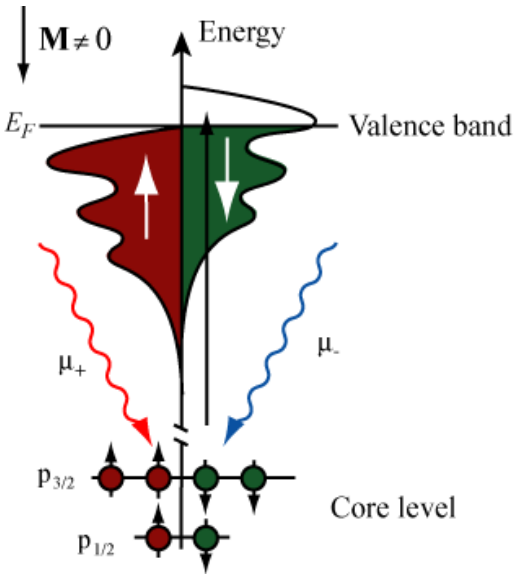

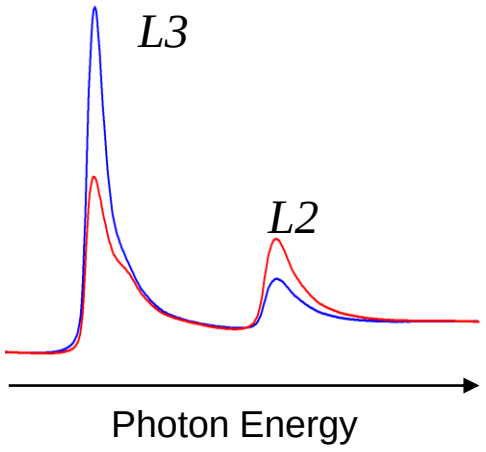

X-rays absorption and X-ray magnetic circular dichroism (XMCD)

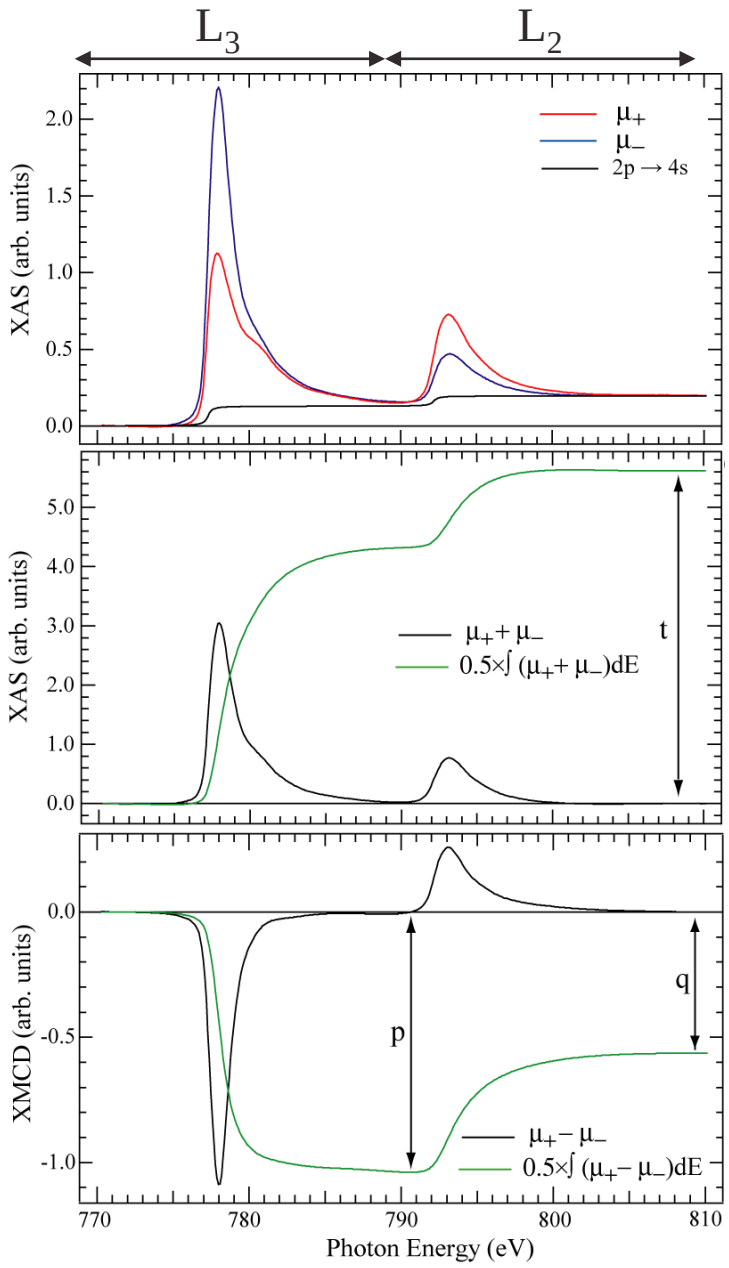

Sum rules for 3d transition metals:

$$L = -\frac{4}{3} h_d \frac{\int_{L3+L2} (\mu_+ - \mu_-) dE}{\int_{L3+L2} (\mu_+ + \mu_-) dE} = -\frac{4}{3} h_d \frac{q}{t}$$

$$S + 7D = -h_d \frac{6\int_{L3} (\mu_+ - \mu_-) dE - 4\int_{L3+L2} (\mu_+ - \mu_-) dE}{\int_{L3+L2} (\mu_+ + \mu_-) dE}$$

$$= -h_d \frac{6p - 4q}{t}$$

h_d -> number of d-holes in the valence band (frequently unknown)
D -> spin dipole moment

$$r = \frac{L}{S + 7D}$$

This value is independent on h_d and can be easily compared among different samples

B. T. Thole *et al.* PRL **68**, 1943 (1992)
P. Carra *et al.* PRL **70**, 694 (1993)

General sum rules

B. T. Thole *et al.* PRL **68**, 1943 (1992)
P. Carra *et al.* PRL **70**, 694 (1993)

Orbital moment L

$$\rho \equiv \frac{\int_{\text{edge}} d\omega(\mu^+ - \mu^-)}{\int_{\text{edge}} d\omega(\mu^+ + \mu^- + \mu^0)} = \frac{1}{2}\,\frac{c(c+1) - l(l+1) - 2}{l(l+1)(4l+2-n)}\,\frac{\langle L_z \rangle}{\hbar}$$

Spin S + magnetic dipole T

$$\delta \equiv \frac{\int_{j_+} d\omega(\mu^+ - \mu^-) - [(c+1)/c]\int_{j_-} d\omega(\mu^+ - \mu^-)}{\int_{j_+ + j_-} d\omega(\mu^+ + \mu^- + \mu^0)} = \frac{l(l+1) - 2 - c(c+1)}{3c(4l+2-n)}\,\frac{\langle S_z \rangle}{\hbar} + \frac{l(l+1)\,[l(l+1) + 2c(c+1) + 4] - 3(c-1)^2(c+2)^2}{6lc(l+1)(4l+2-n)}\,\frac{\langle T_z \rangle}{\hbar}$$

c -> core electron orbital moment
l -> valence electron orbital moment
n -> number of electrons in the valence shell

$L_{2,3}$ edges of 3d metal : *c* = 1 (p states) and *l* = 2 (d states)
$M_{4,5}$ edges of rare earth: *c* = 2 (d states) and *l* = 3 (f states)

$$h_d \propto \int_{L3+L2} (\mu_+ + \mu_- + \mu_0) dE \approx \frac{3}{2} \int_{L3+L2} (\mu_+ + \mu_-) dE$$

Experimentally difficult to measure along the three directions
(α is the quantization axis defined by the external field)

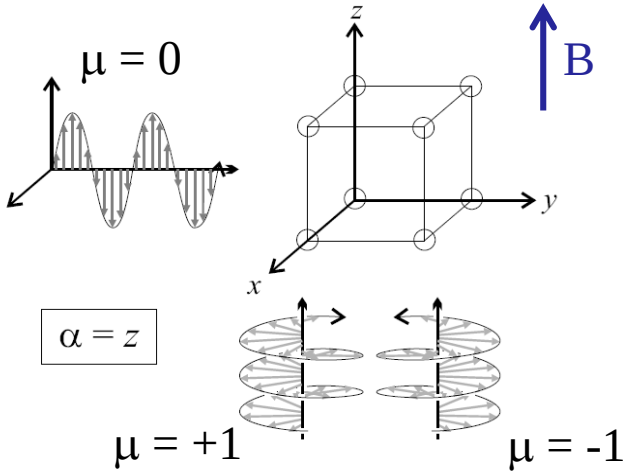

XMCD

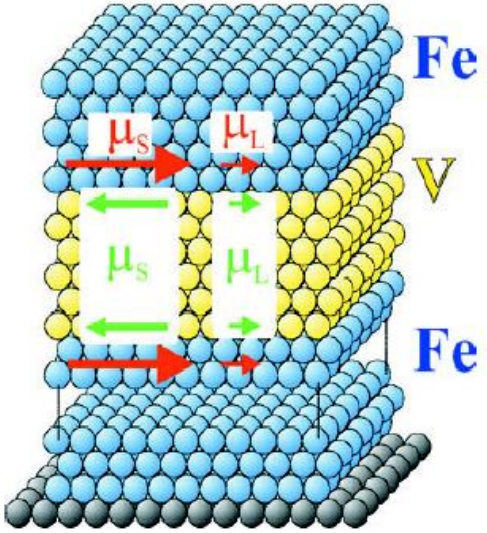

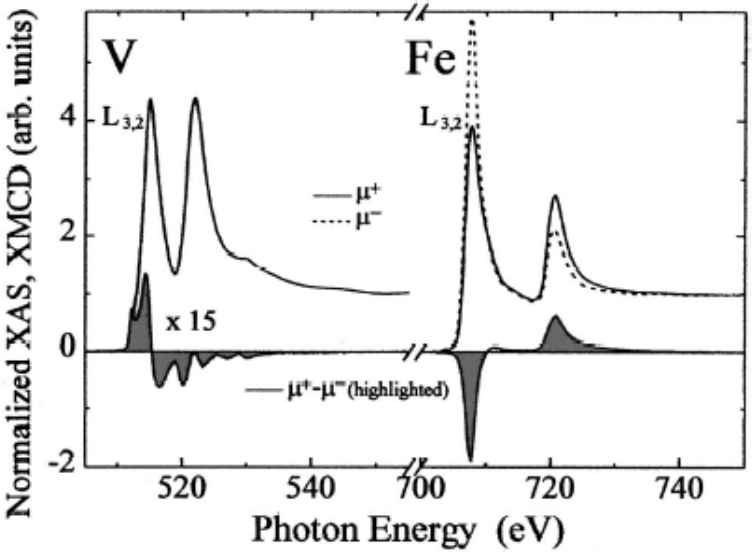

Normalized XAS of L (dashed line) and R (solid line) circularly polarized light and the XMCD at the $L_{2,3}$ edges of V and Fe for a Fe/V4 /Fe(110) trilayer.

Antiferromagnetic coupling: XMCD signal for V and Fe have opposite signs

The induced magnetic moment in the V atoms strongly reduces with increasing the V thickness

Sum rules can not be easily applied due to overlapping between $2p^{1/2}$ and $2p^{3/2}$ states

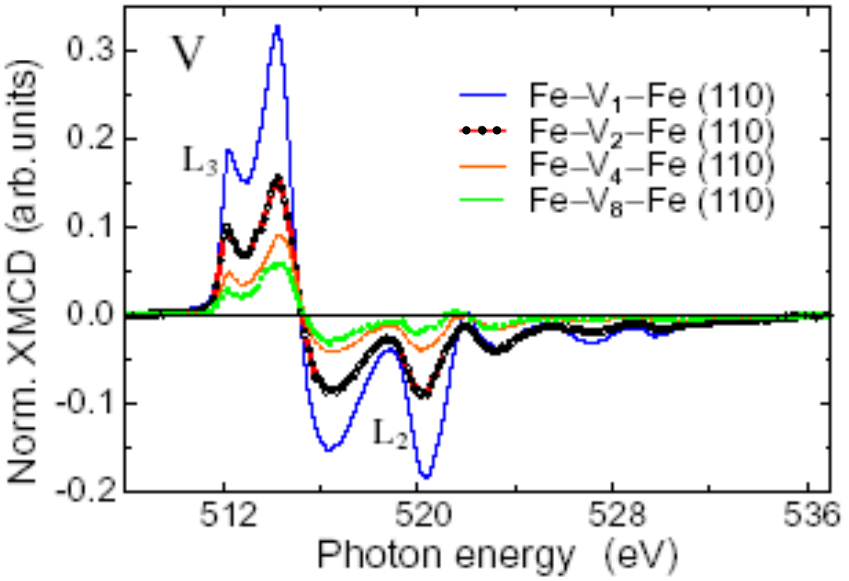

A. Scherz *et al.*, J. Appl. Phys. **91**, 8760 (2002)

Linear dichroism

Dipole selection rules
$\Delta l = 0, \Delta s = 0$

XMLD

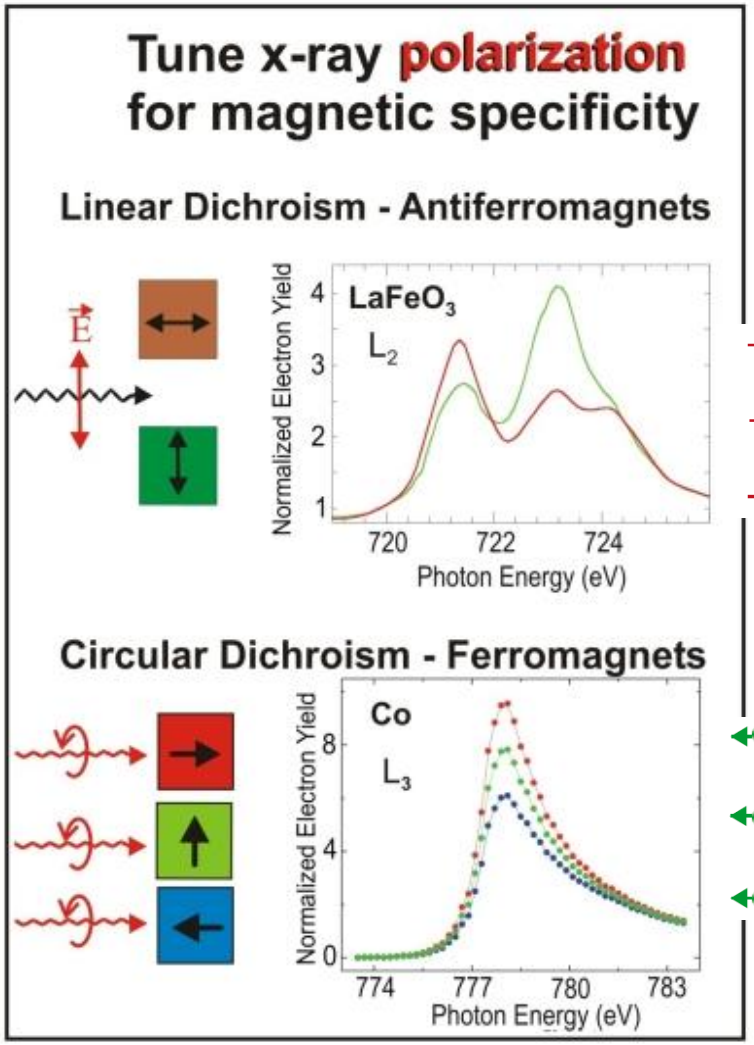

AFM

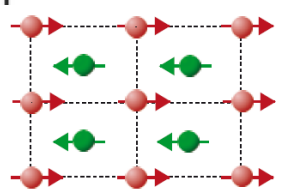

FM

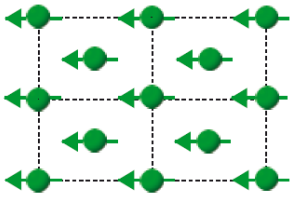

Warning: XNLD
Linear dichroism is also sensible to charge anisotropy (natural dichroism)

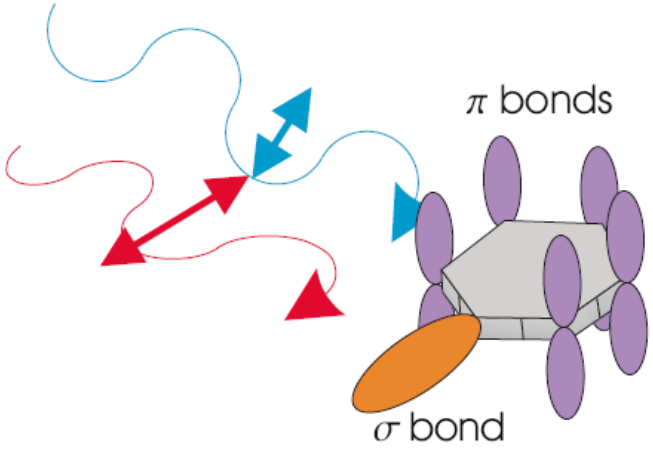

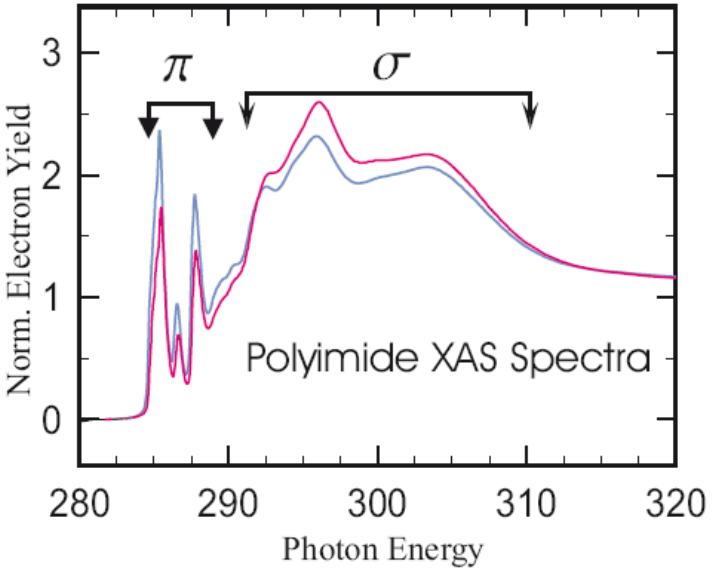

J. Regan, PhD thesis (2001), Stanford university

3d atom on a substrate: electronic hybridization

isotropic:
free magnetic atom

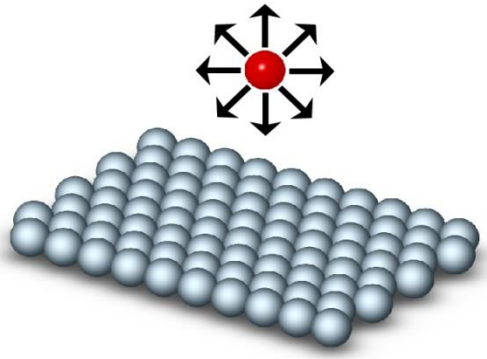

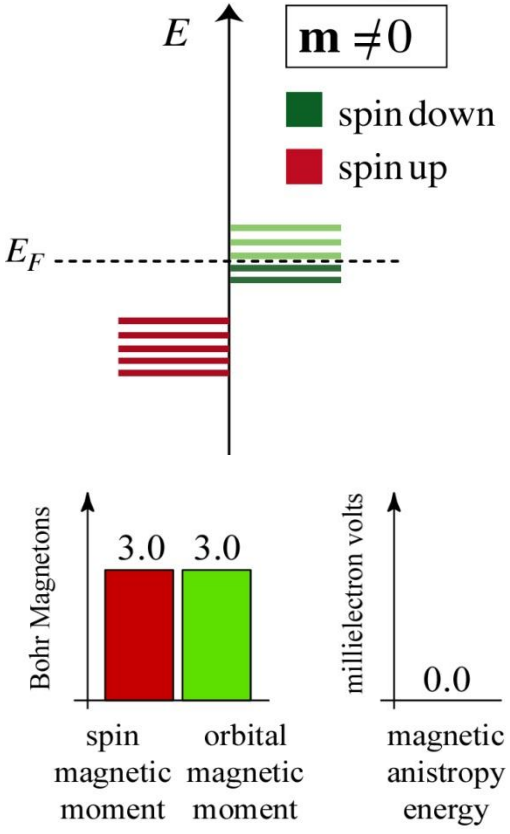

anisotropic:
magnetic atom on a surface

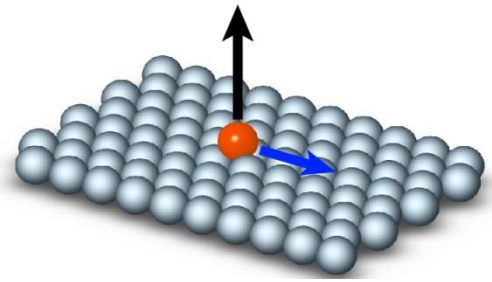

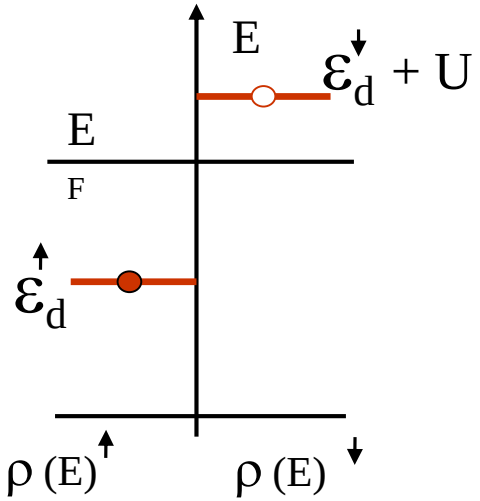

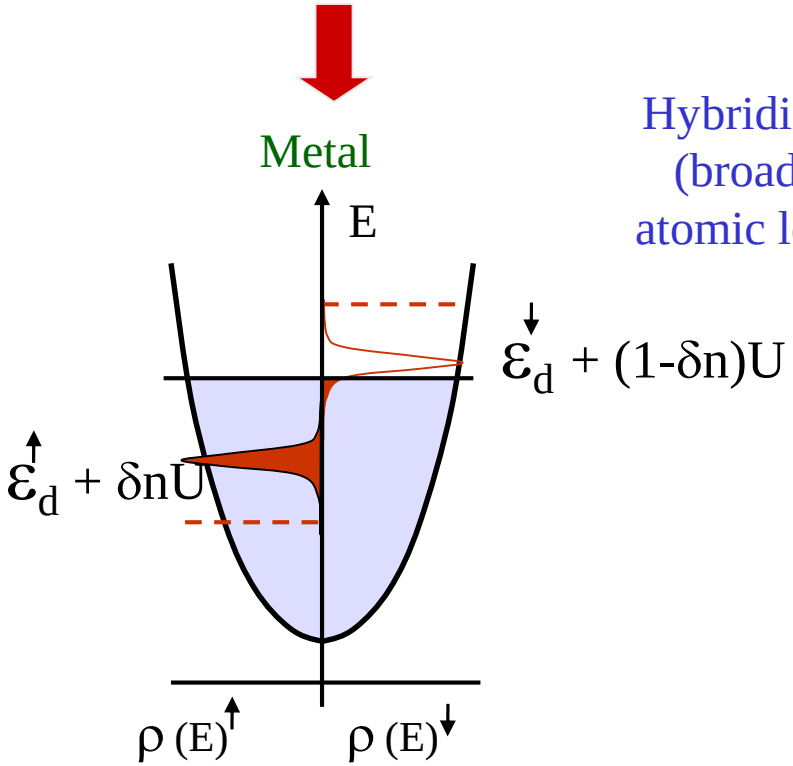

Hybridization with the substrate (broadening of the quantized atomic level and charge transfer)

3d atoms on an sp metal host

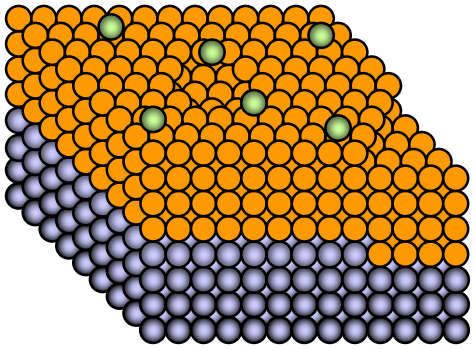

B = 7T

Fe, Co atoms (<0.01 ML)

Cs, K, Na, or Li film

Cu(100)

Spectra are independent on the **B** field orientation: absence of magnetization easy axis

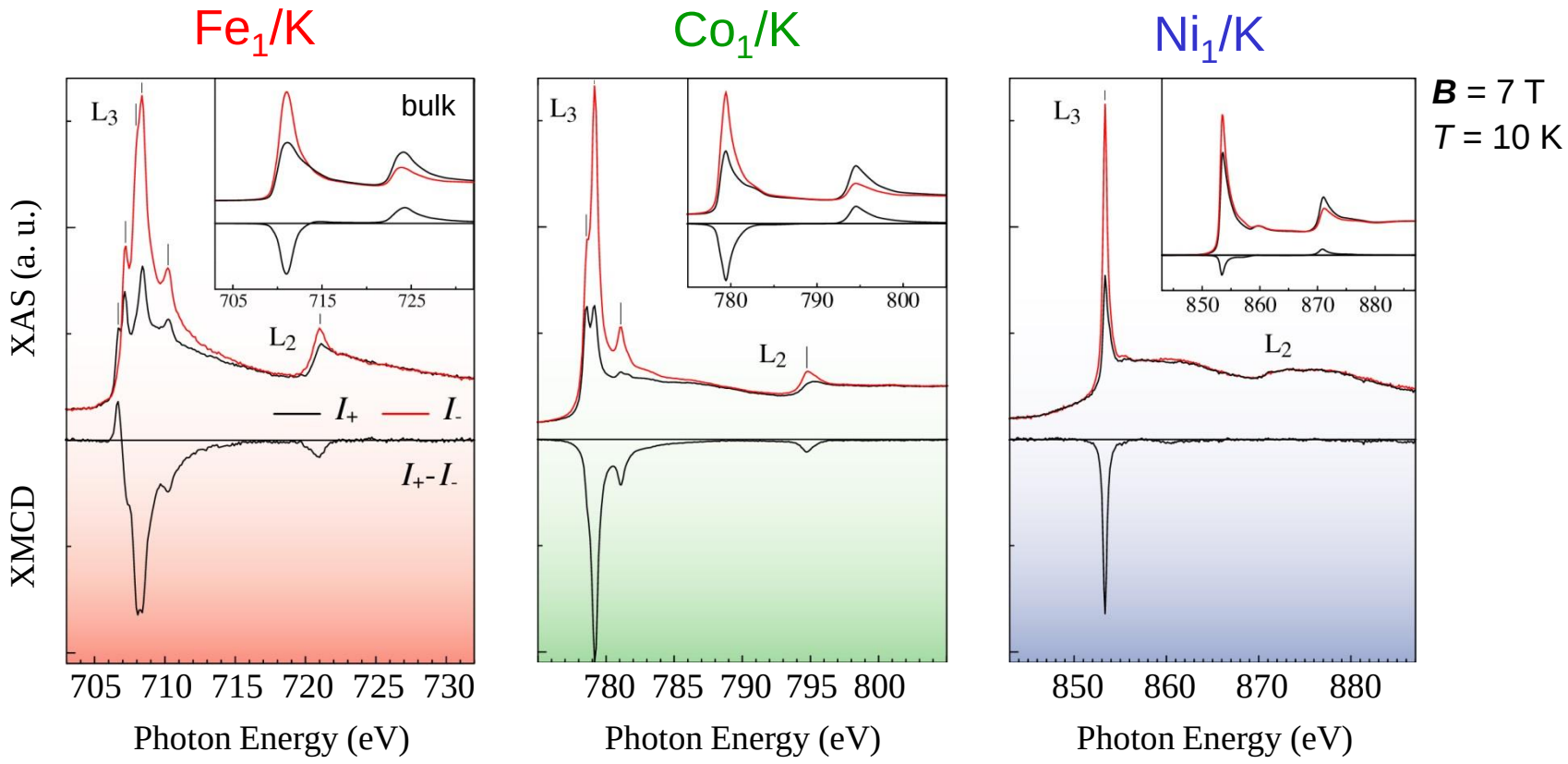

P. Gambardella *et al.* Phys. Rev. Lett. **88**, 047202 (2002)

3d atomic spectra

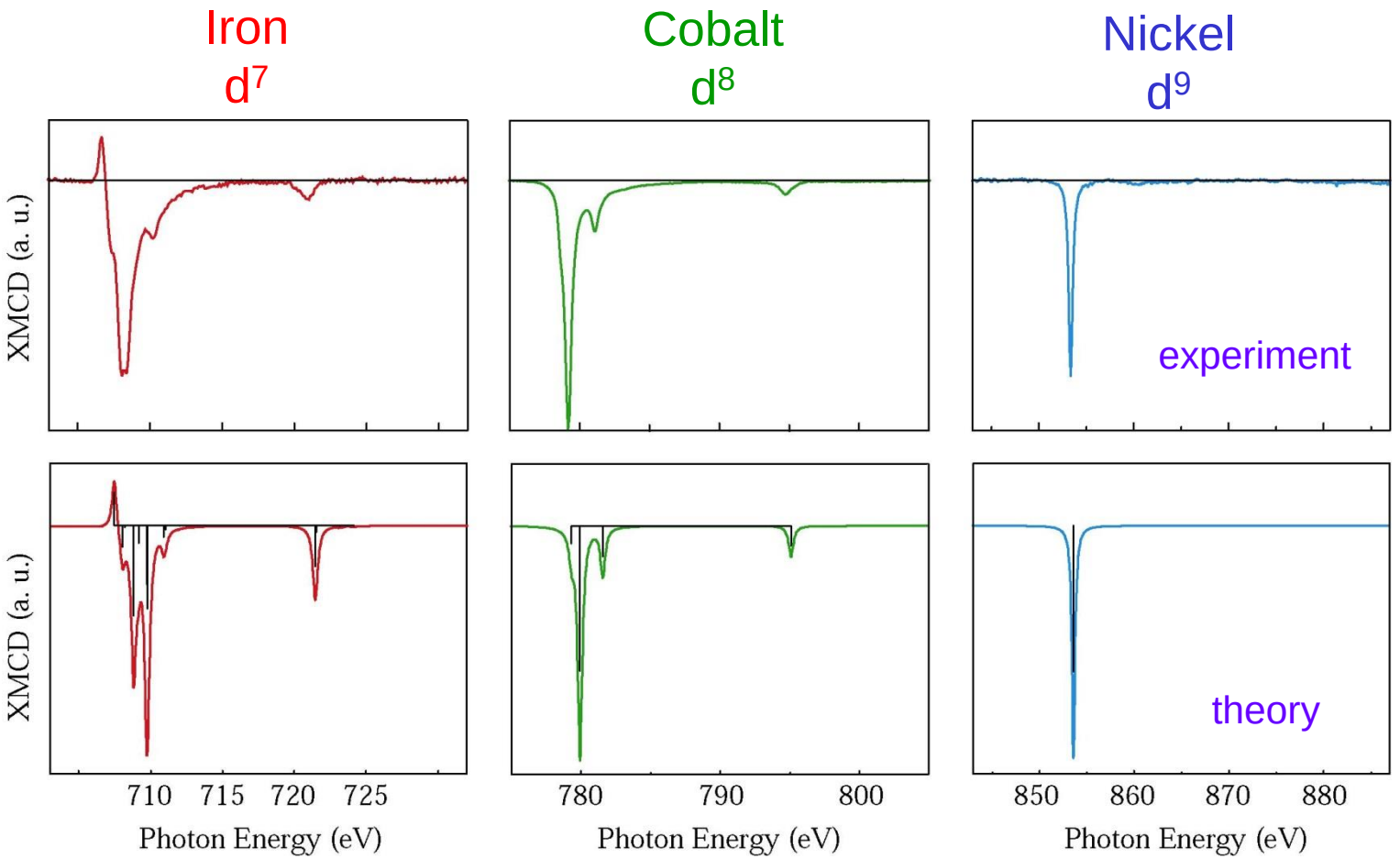

Fe gas phase: d^6 → Fe_1/K: d^7

$m_L = 2 \rightarrow 3\ \mu_B$

$m_S = 4 \rightarrow 3\ \mu_B$

Co gas phase: d^7 → Co_1/K: d^8

$m_L = 3 \rightarrow 3\ \mu_B$

$m_S = 3 \rightarrow 2\ \mu_B$

Ni gas phase: d^8 → Ni_1/K: d^9

$m_L = 3 \rightarrow 2\ \mu_B$

$m_S = 2 \rightarrow 1\ \mu_B$

XMCD multiplet calculations: Hartree-Fock atomic wavefunctions, zero-crystal field limit

G. Van der Laan and B.T. Thole, Phys. Rev. B **43**, 13401 (1991).

Magnetic moment *vs.* substrate electron density

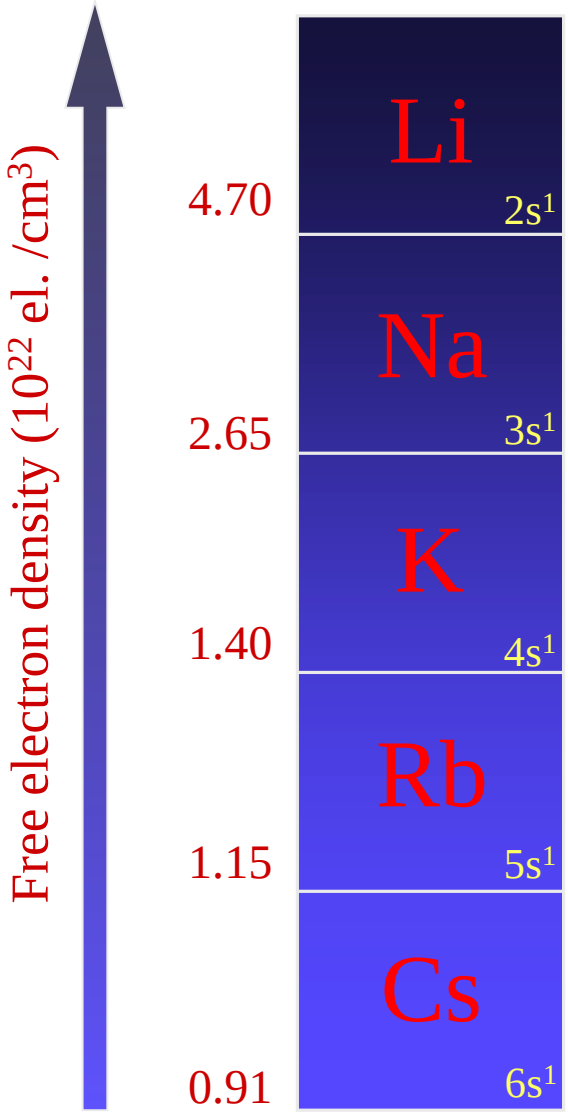

B = 7 Tesla, *T* = 10 K

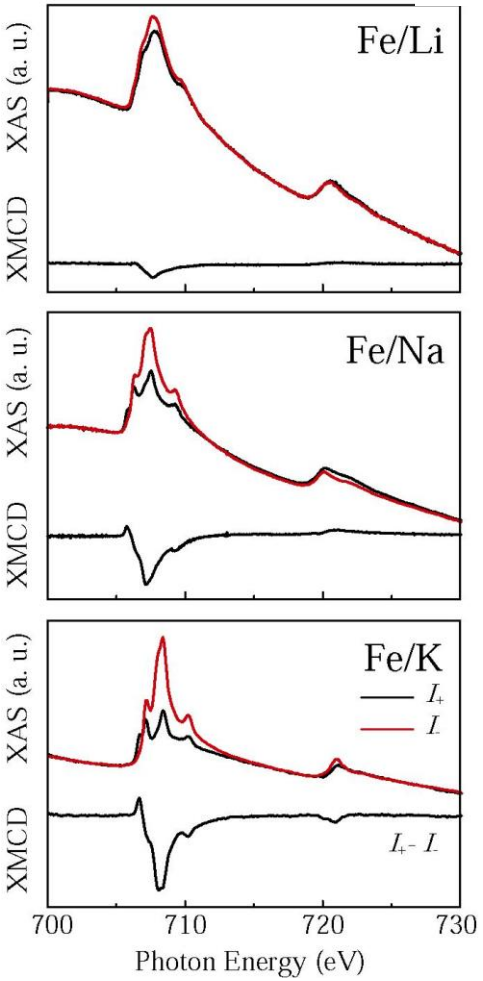

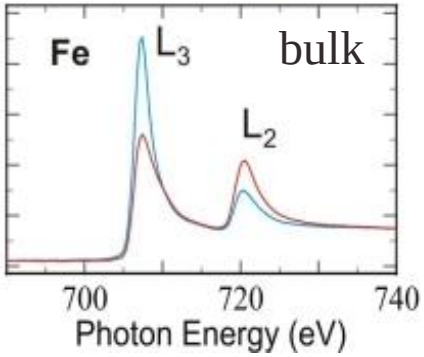

Evolution toward a bulk-like spectrum

The magnetic moment (amplitude of the XMCD signal) decreases increasing the substrate electron density

3d clusters on a sp metal host: magnetic moment *vs.* cluster size

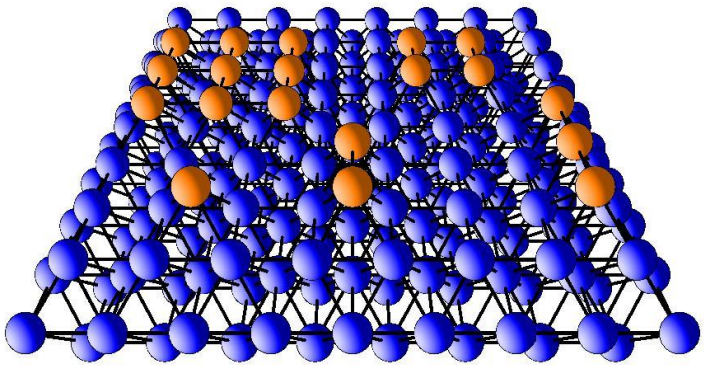

individual atoms ← | → clusters

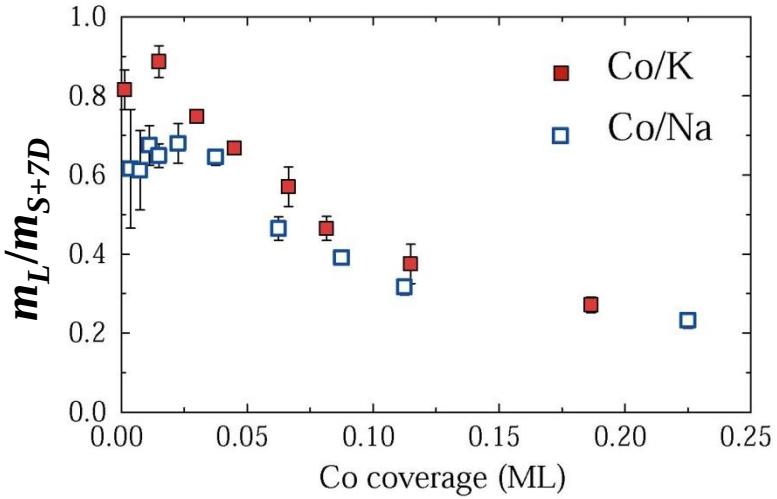

The XMCD lineshape changes with m_L, m_S

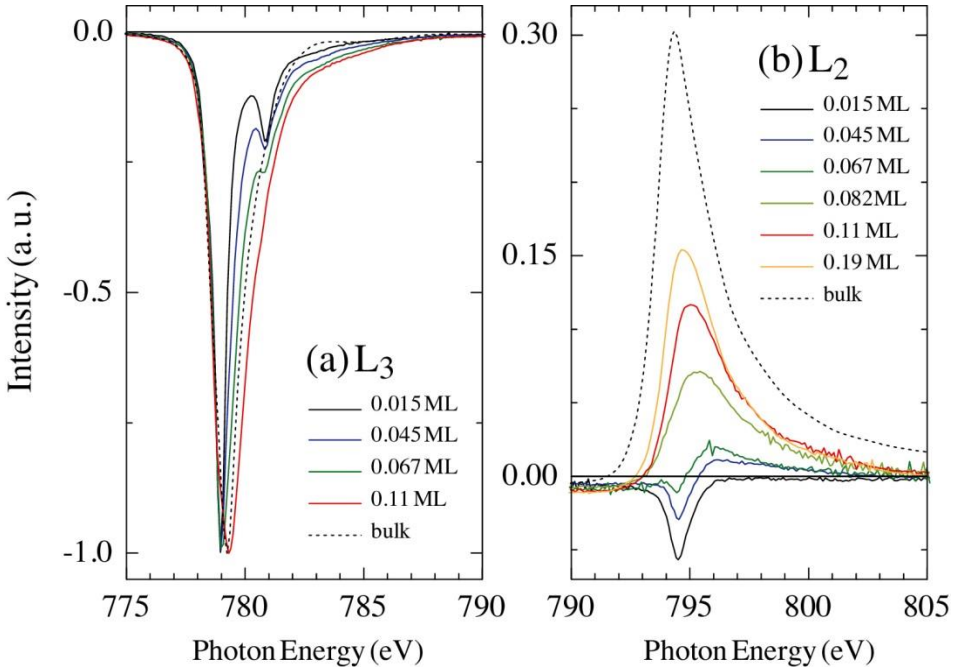

Hund's limit for d^8 ion: $m_L/m_{S+7D} = 1$

Bulk Co hcp: $m_L/m_S = 0.1$

7D ~ 0 in bulk

P. Gambardella *et al.*, Phys. Rev. Lett. **88**, 047202 (2002)

Free atom: magnetic moment *vs.* magnetic field

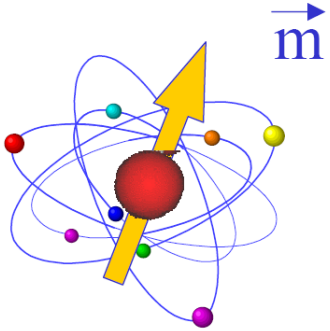

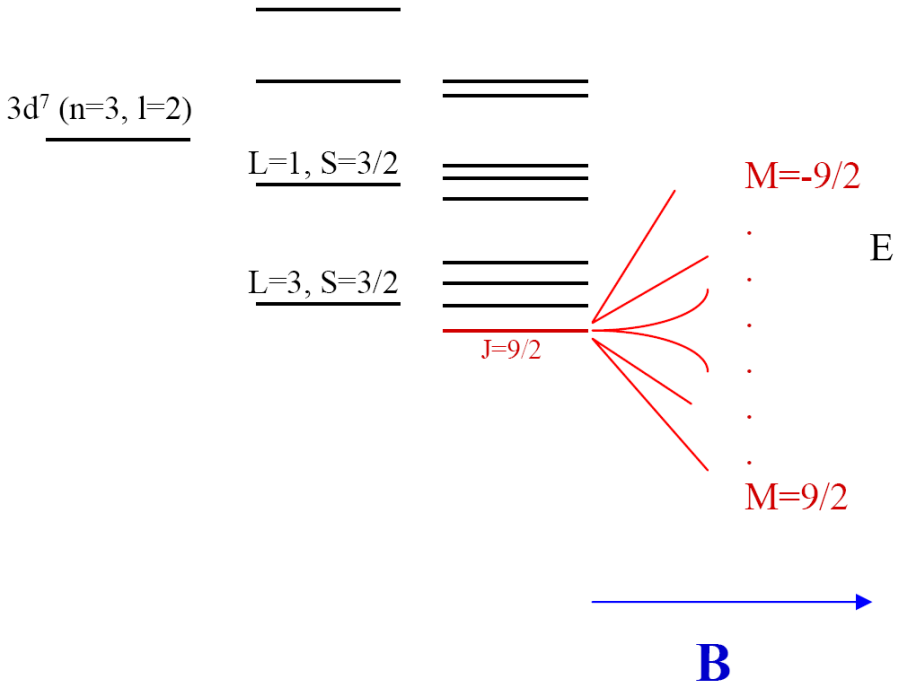

$$E = -\mathbf{m}_J \cdot \mathbf{B} = -\mu_B g_J M B$$

Ground state of a $3d^7$ ion (e.g., Co^{2+})

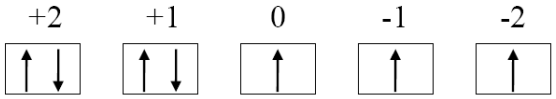

$L = 3,\ S = 3/2,\ J = 9/2$

$m_L = -L\ \mu_B = -3\ \mu_B$,

$m_S = -2\ S\ \mu_B = -3\ \mu_B$,

$$\langle m \rangle = N \frac{\sum_{M=-J}^{J} m_J e^{-\frac{\mu_B g_J B M}{kT}}}{\sum_{M=-J}^{J} e^{-\frac{\mu_B g_J B M}{kT}}} = N \frac{\sum_{M=-J}^{J} \mu_B g_J M\, e^{-\frac{\mu_B g_J B M}{kT}}}{\sum_{M=-J}^{J} e^{-\frac{\mu_B g_J B M}{kT}}} = N \mu_B g_J J\, B_J\left(\frac{\mu_B g_J J B}{kT}\right)$$

Brillouin function

$$B_J(x) = \frac{2J+1}{2J}\coth\left(\frac{2J+1}{2J}x\right) - \frac{1}{2J}\coth\left(\frac{1}{2J}x\right)$$

P. Gambardella *et al.*, Phys. Rev. Lett. **88**, 047202 (2002)

magnetic moment: classic *vs.* quantum description

quantum

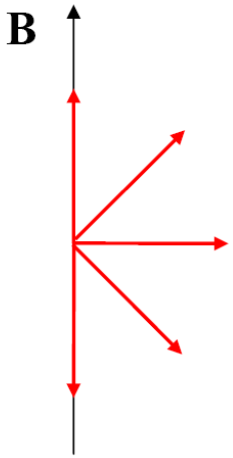

classic

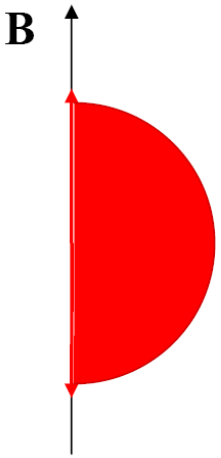

$$M = M_{SAT}\frac{\int_0^{2\pi} d\vartheta \int_0^{\pi} d\varphi \sin\varphi\cos\vartheta\, e^{-\frac{E}{k_B T}}}{\int_0^{2\pi} d\vartheta \int_0^{\pi} d\varphi \sin\varphi\, e^{-\frac{E}{k_B T}}}$$

$$m = L + S$$

$$\langle m \rangle = Nm\,L\left(\frac{mB}{kT}\right) \qquad L(x) = \coth(x) - \frac{1}{x}$$

Langevin function

$E = -\mathbf{m}_J \cdot \mathbf{B} = -\mu_B g_J M B$ $\qquad$ $E = -\mathbf{m}_J \cdot \mathbf{B} = -mB\cos\theta$

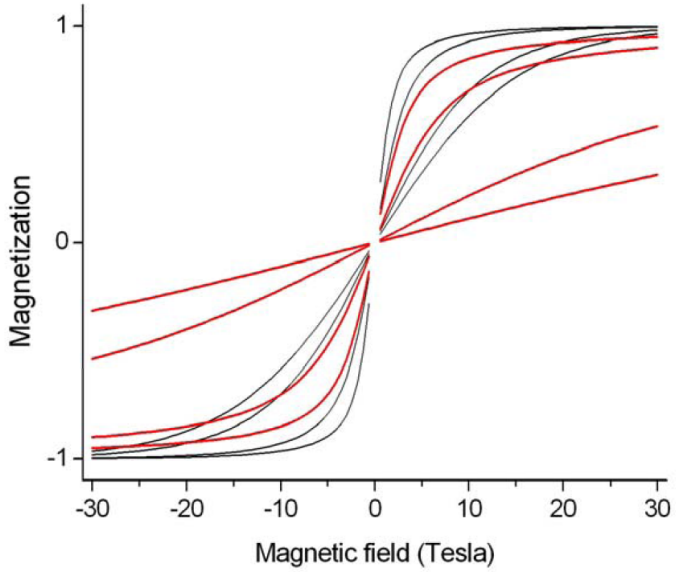

Brillouin	Langevin
J=10	m=10
J=5	m=5
J=1	m=1
J=1/2	m=1/2

$$\chi = \frac{\partial\langle m\rangle}{\partial H} = N\frac{(\mu_B g_J)^2 J(J+1)}{3kT}$$

$$\chi = \frac{\partial\langle m\rangle}{\partial H} = N\frac{m^2}{3kT}$$

magnetic moment *vs.* magnetic field: Fe on K

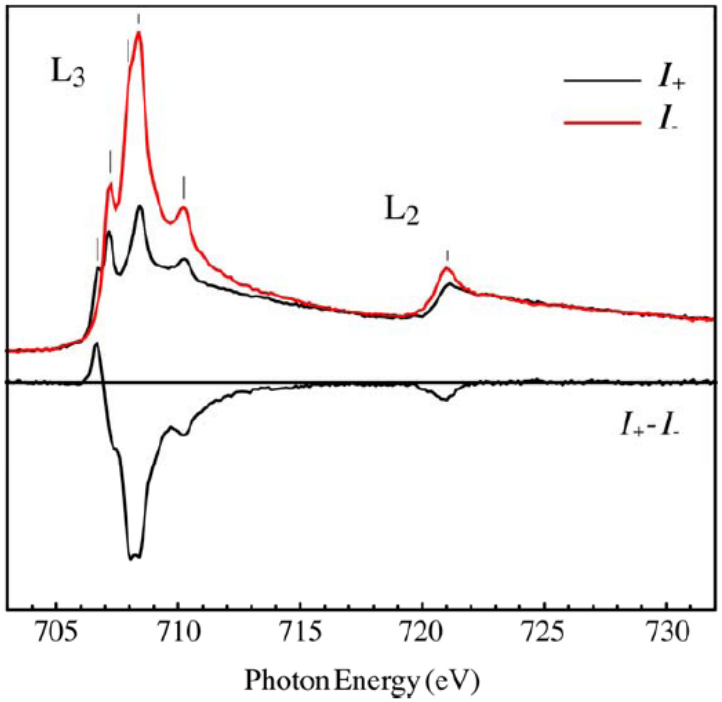

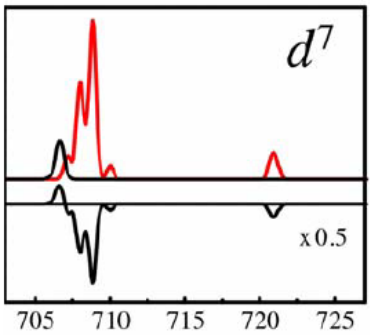

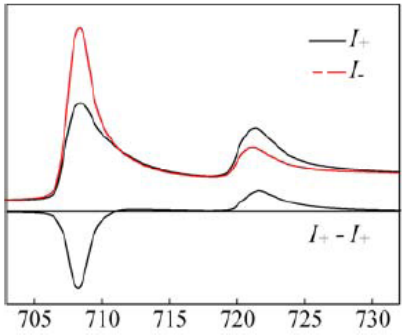

Atomic-like Fe orbitals

Fe $d^6 \rightarrow d^7$.

$L = 3, S = 3/2, J = 9/2 \rightarrow m_{at} = 6.6\ \mu_B$

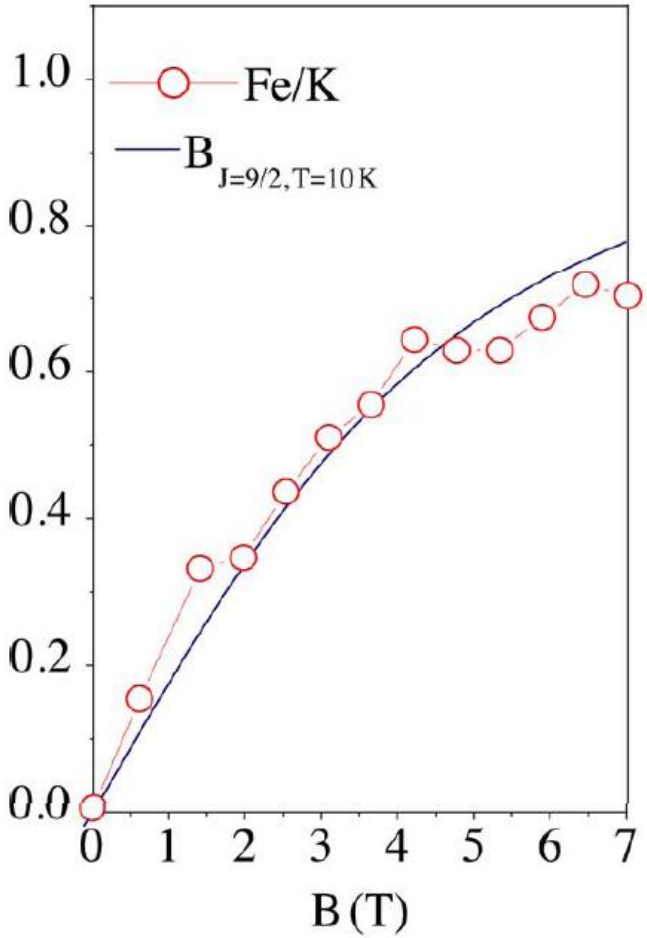

P. Gambardella *et al.*, Phys. Rev. Lett. **88**, 047202 (2002)

3d atoms on an sd metal host: Co on Pt(111)

Spin-orbit interaction between Co wave functions and substrate d-states

- Spectra depend on the **B** field orientation: out-of-plane magnetization easy axis
- No multiplets: bulk-like spectrum

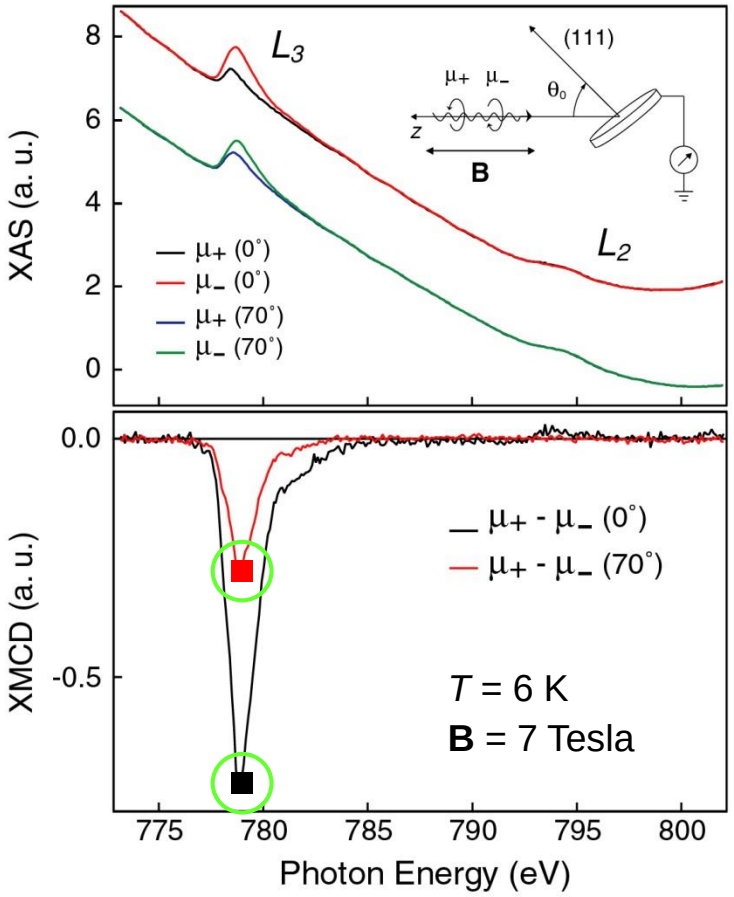

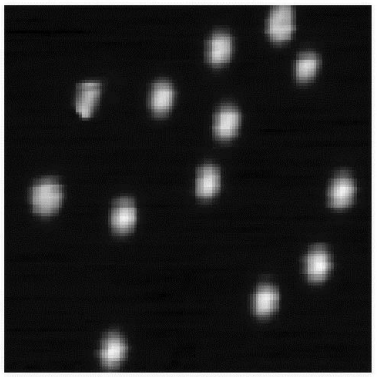

STM image 85 x 85 Å^2

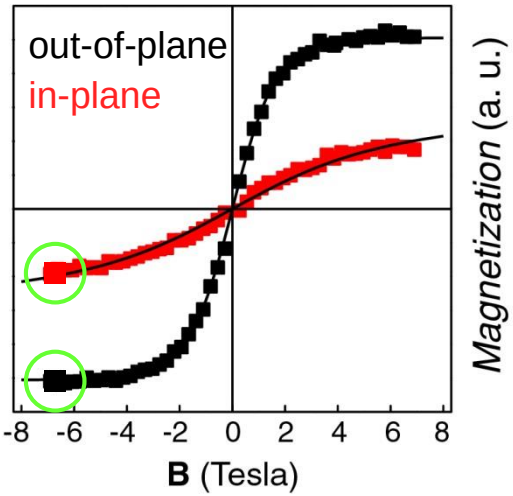

$$\langle \mathrm{m} \rangle = \mathrm{Nm} \frac{\int_0^{2\pi} d\varphi \int_0^{\pi} d\theta \ \sin\theta\cos\theta \ \mathrm{e}^{-\Delta E(\theta,\varphi)/\mathrm{k}T}}{\int_0^{2\pi} d\varphi \int_0^{\pi} d\theta \ \sin\theta \ \mathrm{e}^{-\Delta E(\theta,\varphi)/\mathrm{k}T}}$$

P.Gambardella et al., *Science* **300**, 1130 (2003).

Record (for more than a decade) MAE for a single atom

Co on Pt(111)

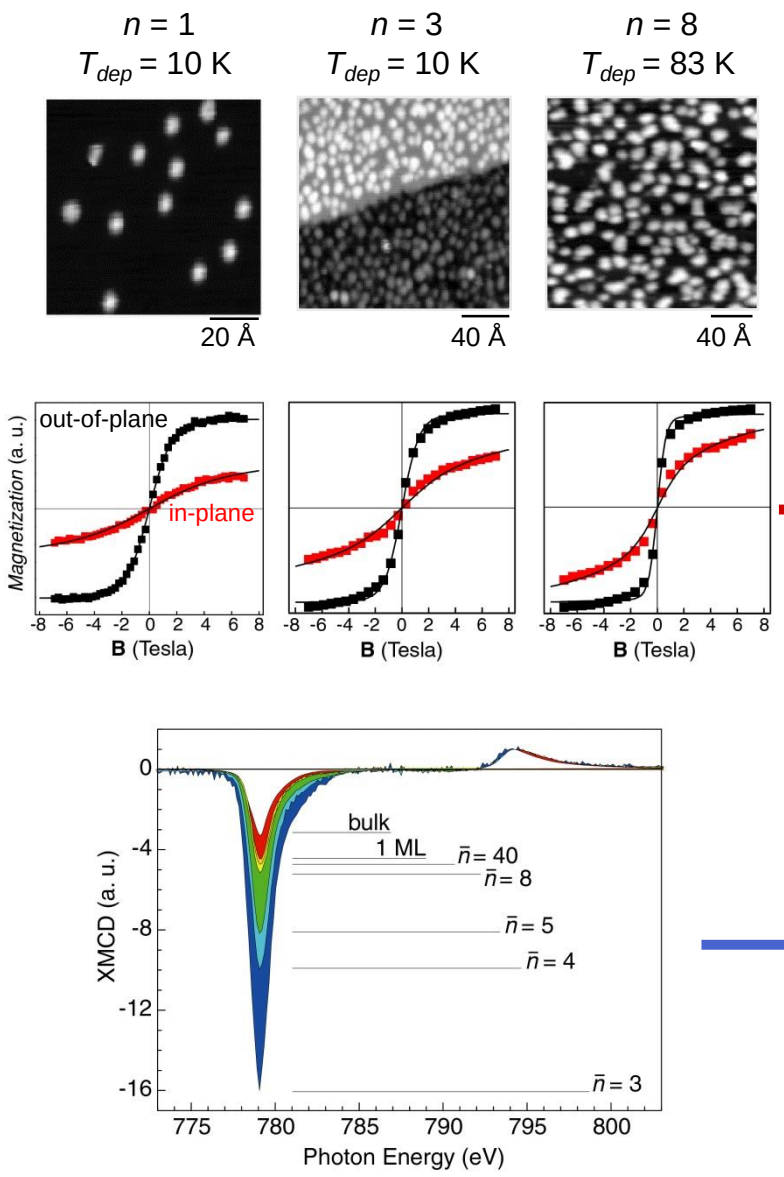

Co particles on Pt(111) with average size *n*

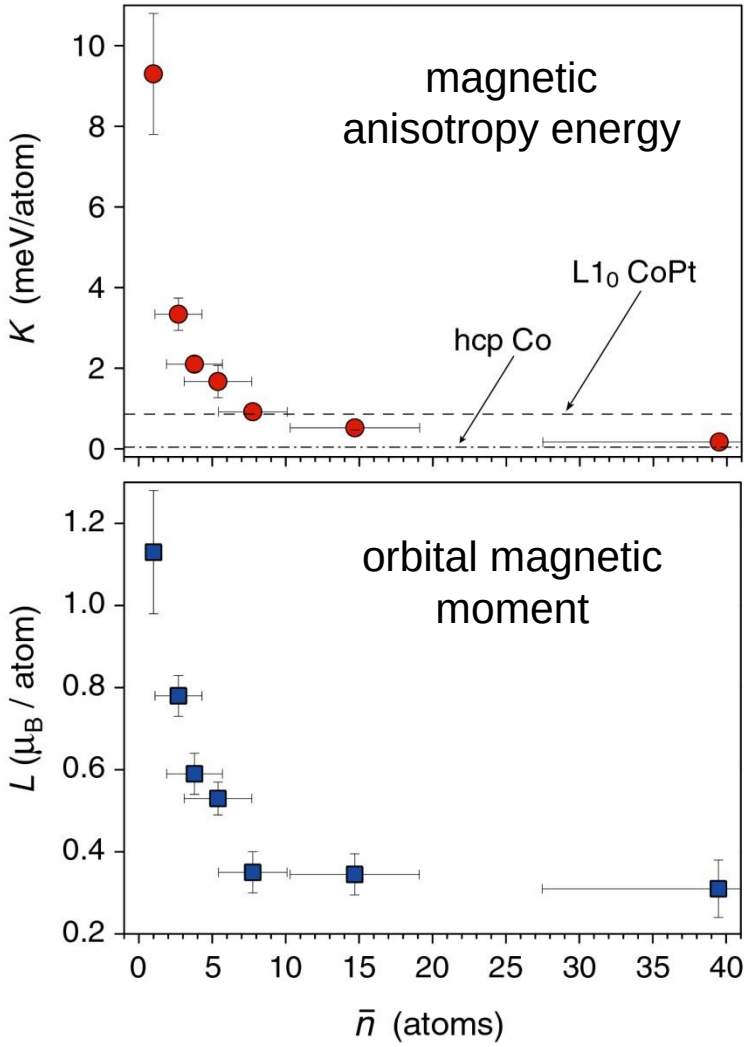

P.Gambardella et al., *Science* **300**, 1130 (2003).

Co on Pt(111): origin of the high MAE

a) CF (C_{3v}) is not enough to explain the (former) record MAE -> K ~ ξ/4 ΔL but ΔL is too small
b) There is a strong hybridization with the Pt(111) substrate

Local μ_{spin} at Co atoms and at substrate atoms for Co clusters of 1–7 atoms

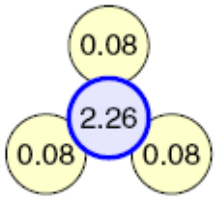

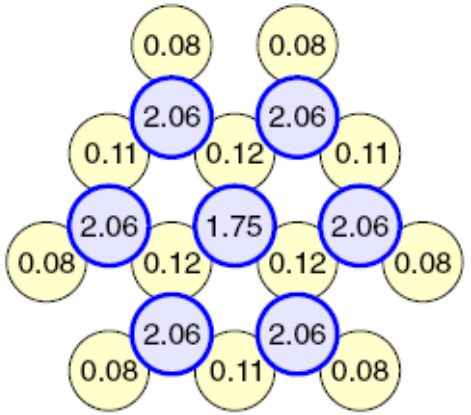

Co atom

Pt atom

Spin moment induced in the Pt substrate:
The induced moment is small but ξ_{Pt} is large -> the substrate contribute to the MAE

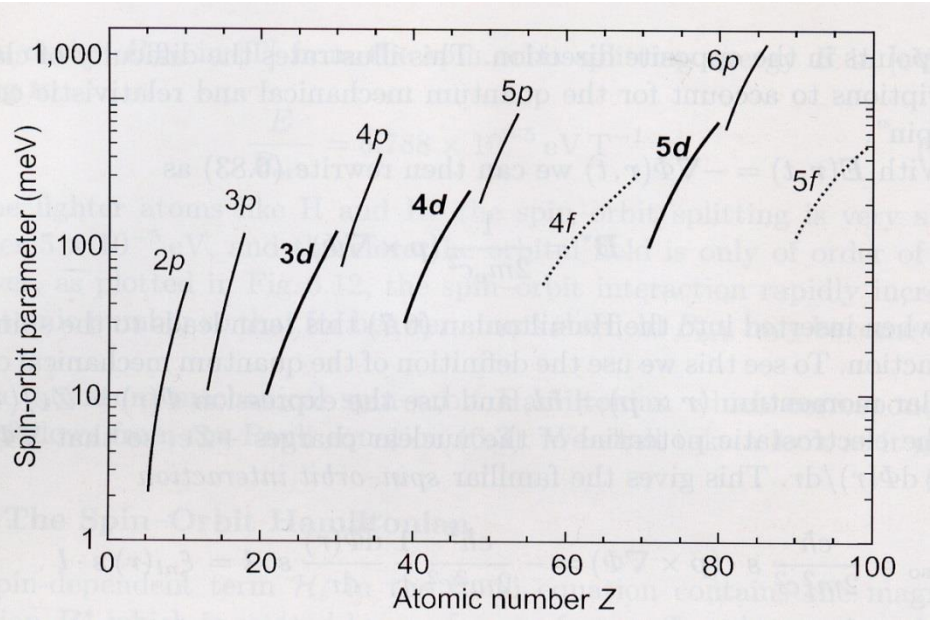

O. Sipr *et al.*, J. Phys.: Condens matter **19**, 096203 (2007).

Magnetic moments and magnetic anisotropy: from atom to bulk

Co/Pt(111)

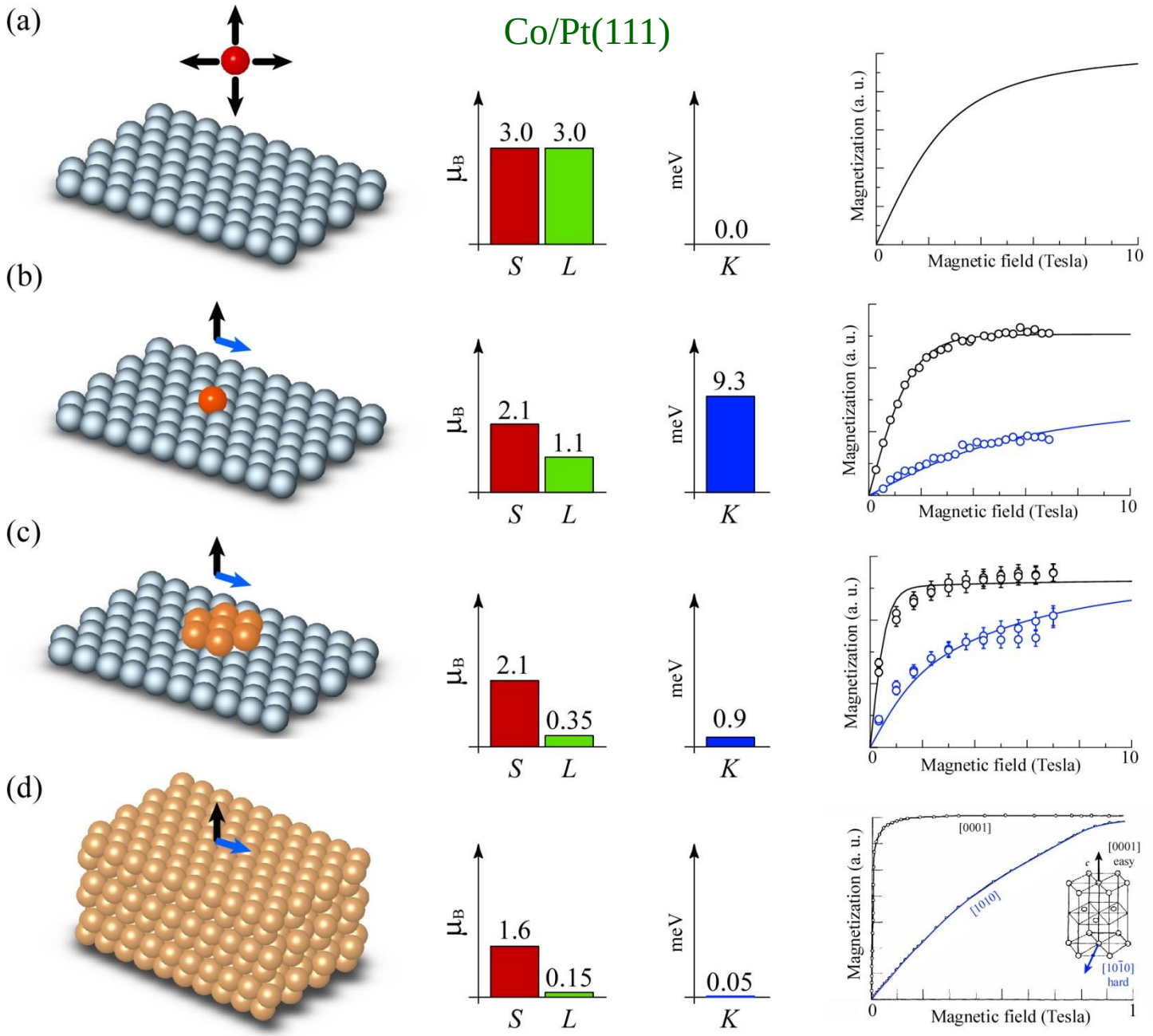

Insulating substrates

$Cu_2N/Cu(001)$

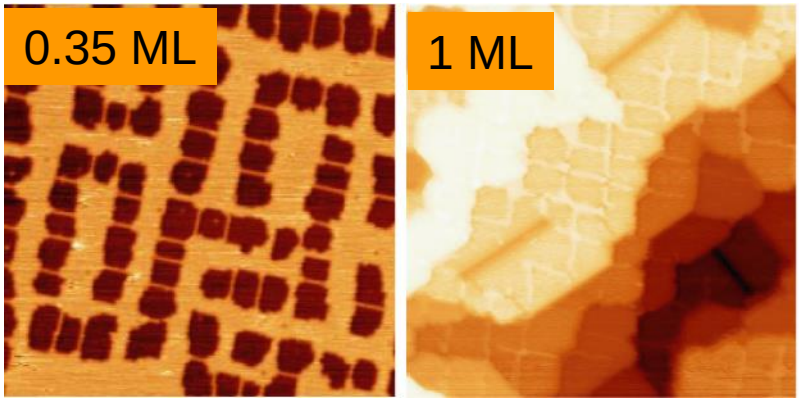

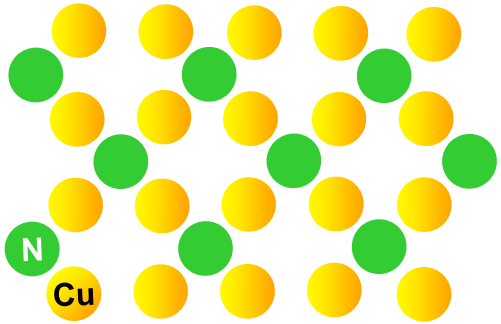

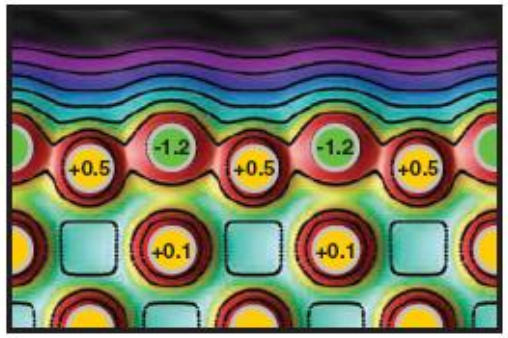

Hirjibehedin *et al.*, Science **317**, 1199 (2007)

Sputtering with N at RT and annealing @ 600 K for 2 min

1 ML thick

band gap of 4 eV Ruggiero *et al.*, APL **91**, 253106 (2007)

MgO/Ag(100)

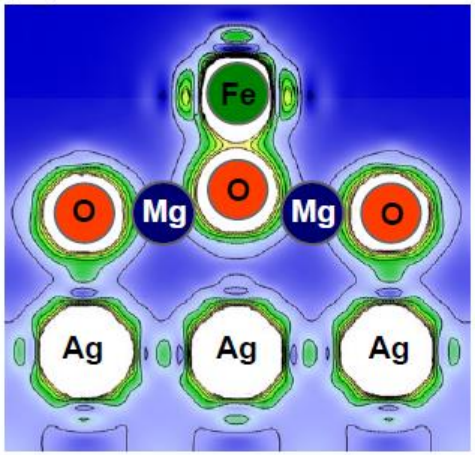

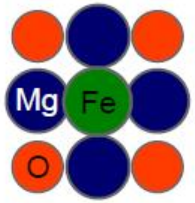

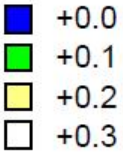

MgO band gap of 8 eV

S. Schintke, *et al.* Phys. Rev. Lett. **87**, 276801 (2001)

Fe and Co atoms on $Cu_2N/Cu(001)$

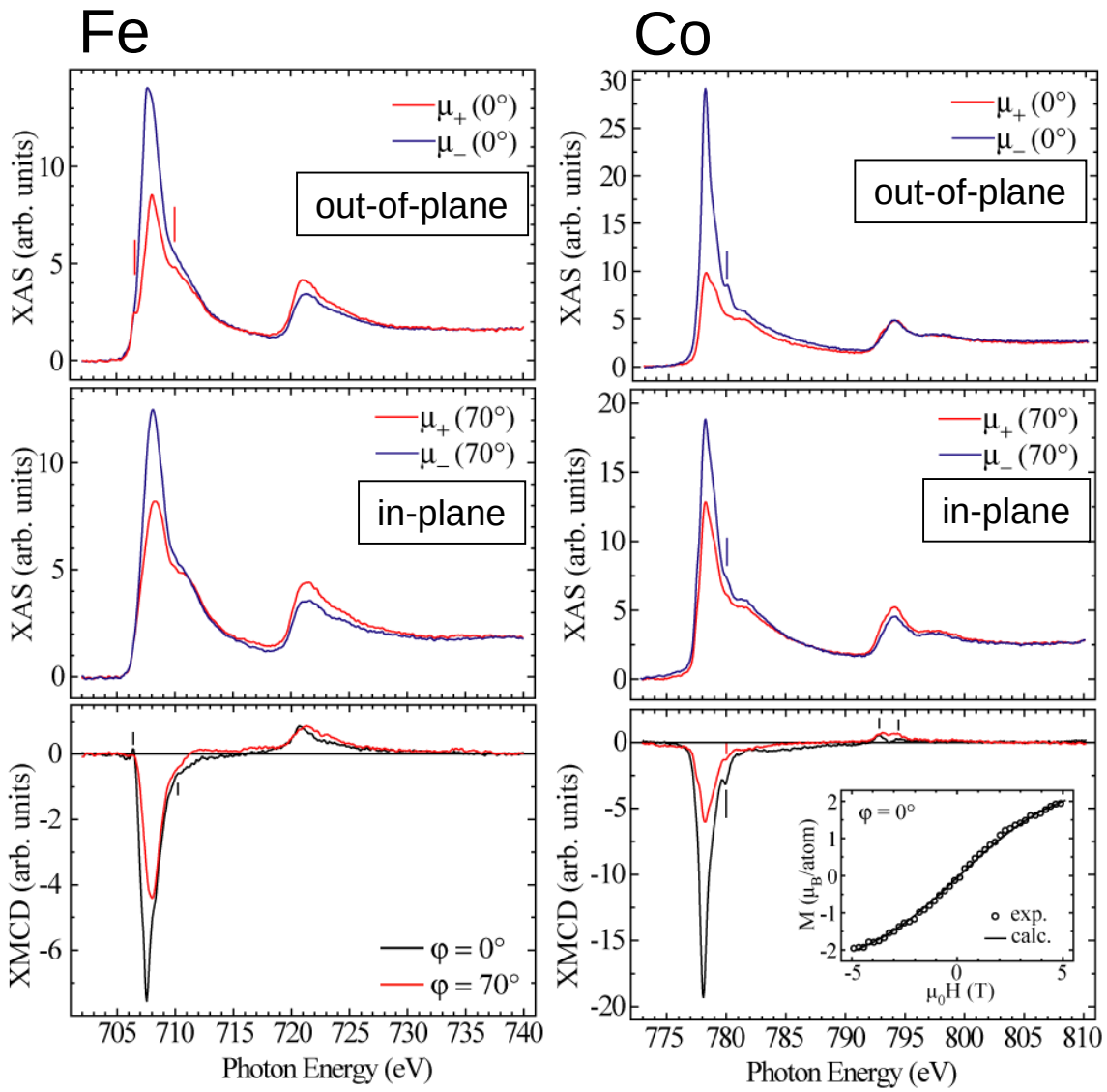

		r	*L*	*S+7D*
Fe	0°	0.24	0.50	2.06
	70°	0.04	0.06	1.75
Co	0°	0.62	1.20	1.95
	70°	0.41	0.42	1.02

- Fe & Co decoupled from Cu(001)
- Large orbital moment
- Easy axis:
  out-of-plane for both elements

B = 5 T and T = 8 K

A. Lehnert, *EPFL thesis n° 4411* (2009)

Co atoms on MgO/Ag(100)

Fe

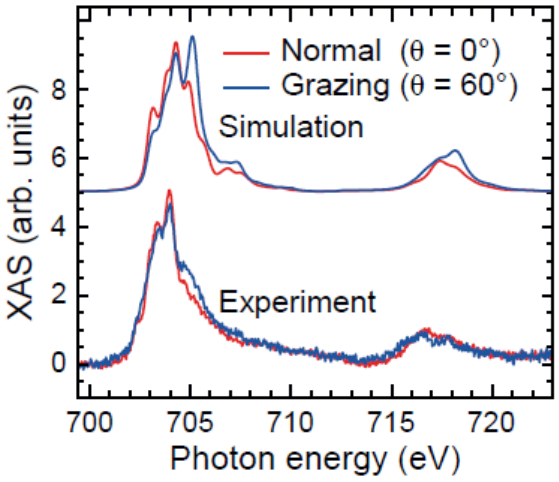

(b)

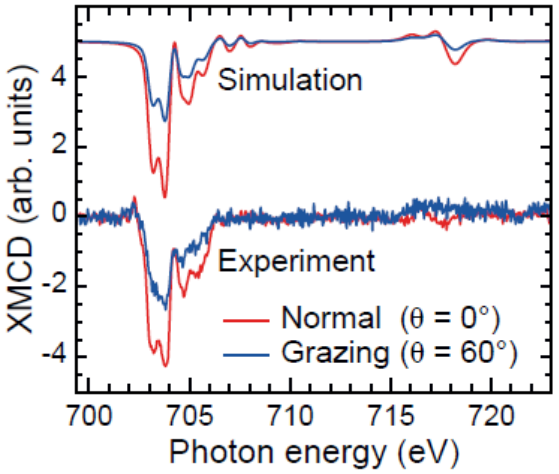

Co

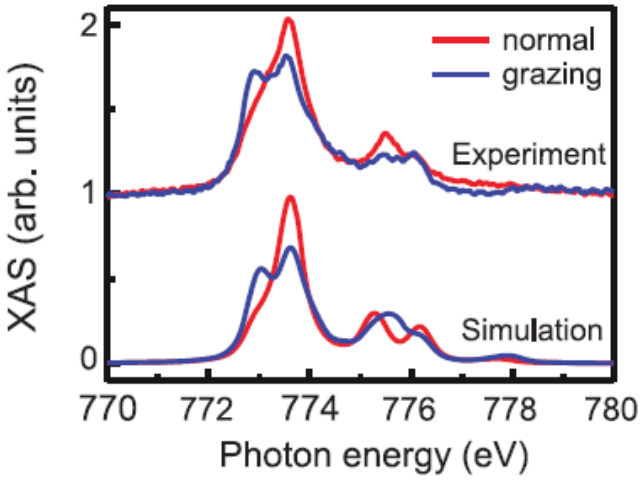

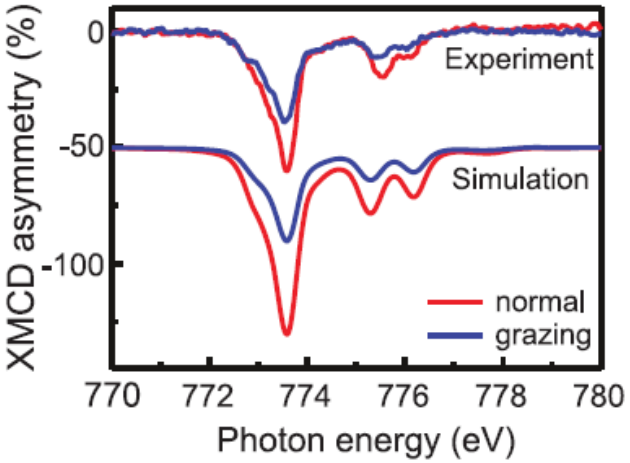

- Fe & Co decoupled from Ag(100): Spectra with multi-peaks

- atomic like orbital moments:
  - Co -> L = 2.5 μ_B
  - Fe -> L= 1.25 μ_B

- Easy axis: out-of-plane for both elements

B = 7 T and T = 2 K

I.G. Rau *et al. Science* 988, **344** (2014);
S. Baumann *et al.* Phys. Rev. Lett. **115**, 237202 (2015).

Theoretical maximum MAE for Co atoms on MgO/Ag(100)

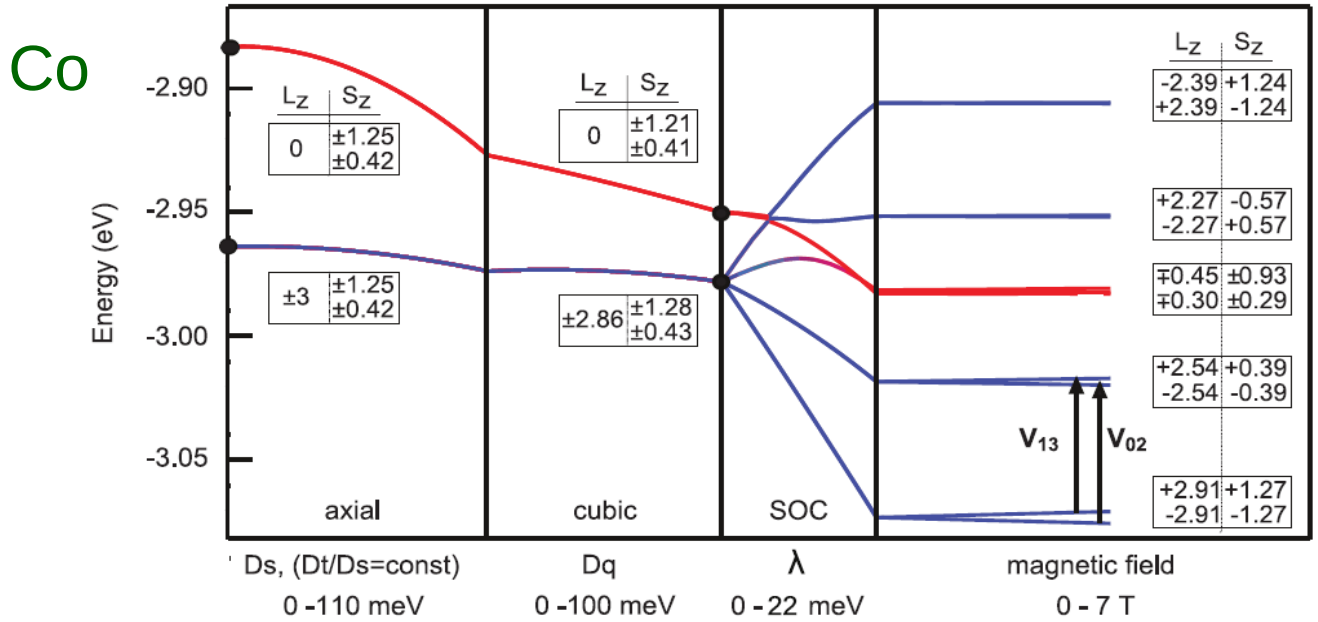

$\Delta E = \lambda L \Delta S$
$= 58$ meV

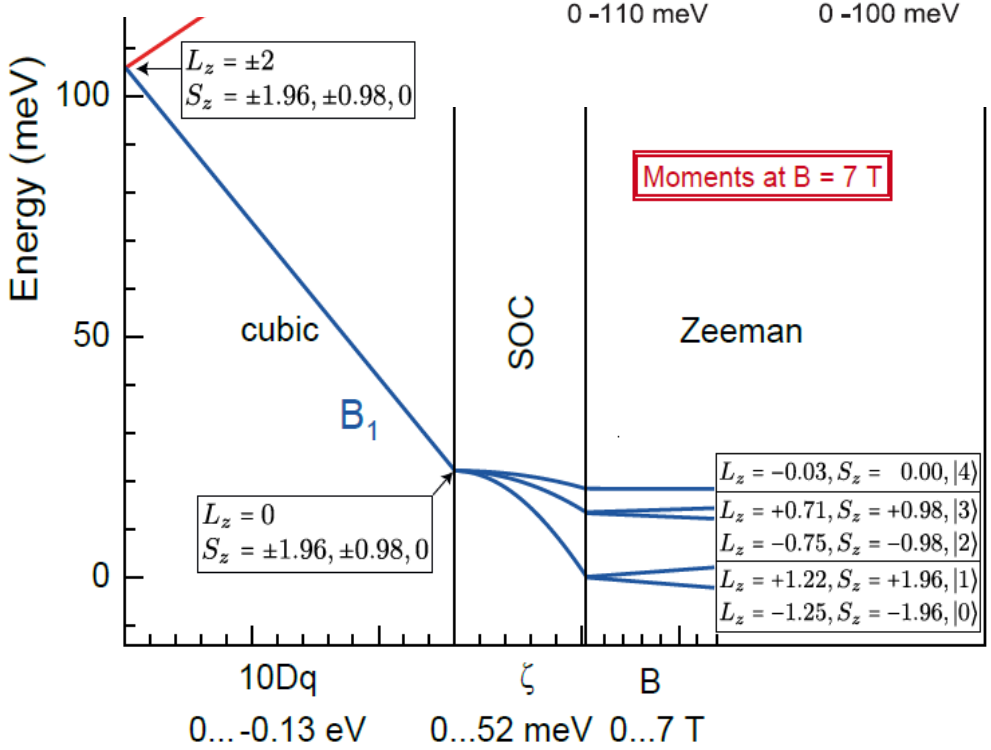

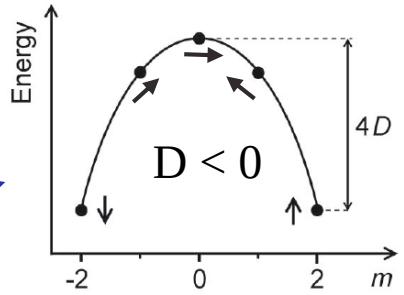

I.G. Rau *et al. Science* 988, **344** (2014);
S. Baumann et al. .....

Excitation by means of STM

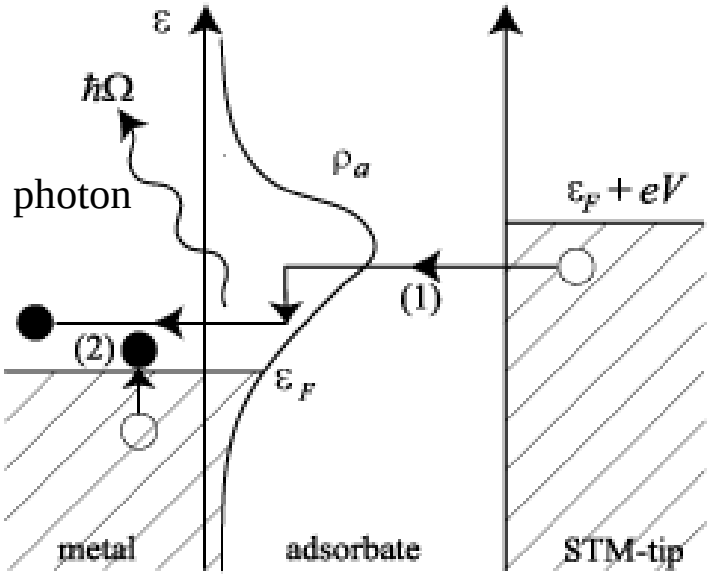

An inelastic tunneling process requires energy transfer between the tunneling electron and the sample. Because this energy is quantized, inelastic channels cannot contribute to the total tunneling current if the bias potential is lower than the quantization energy.

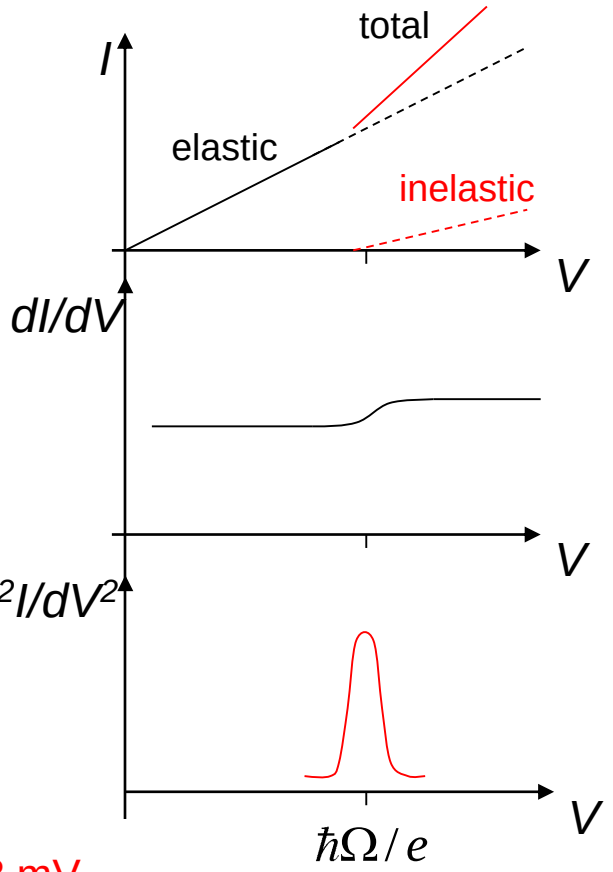

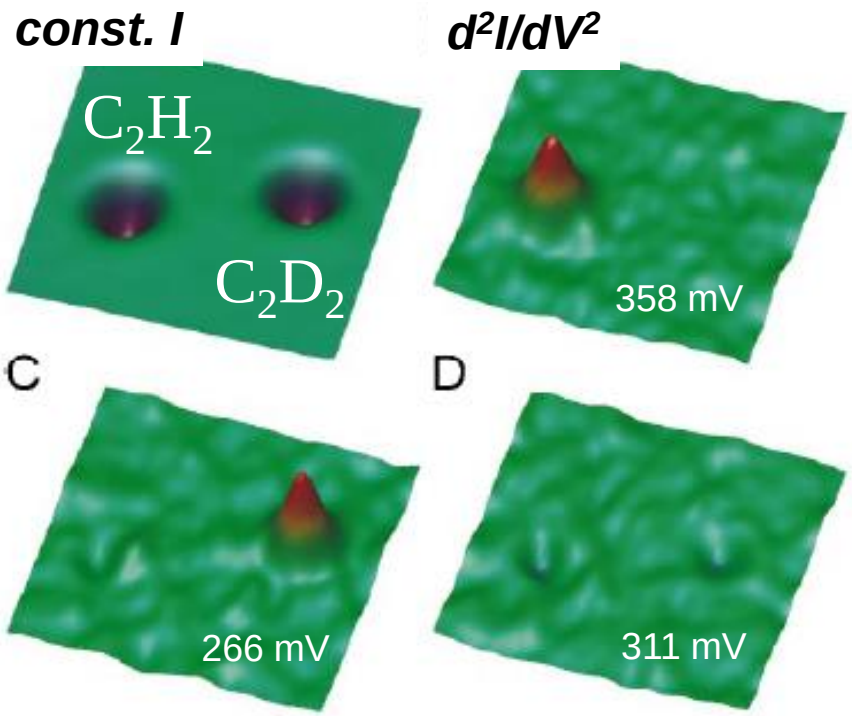

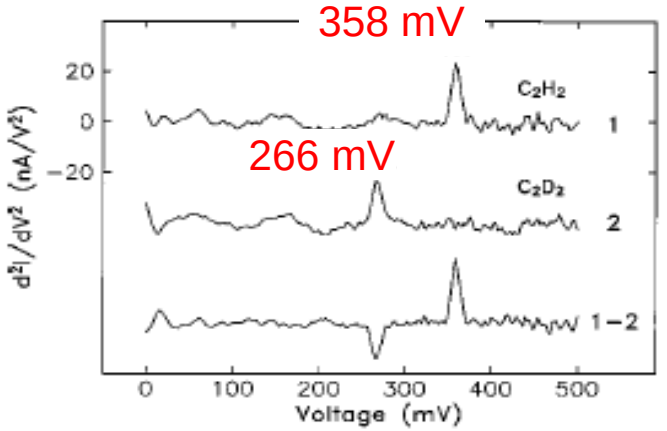

B. C. Stipe, *et al.* Phys. Rev. Lett **82**, 1724 (1999)

Spin-flip excitation by means of STM

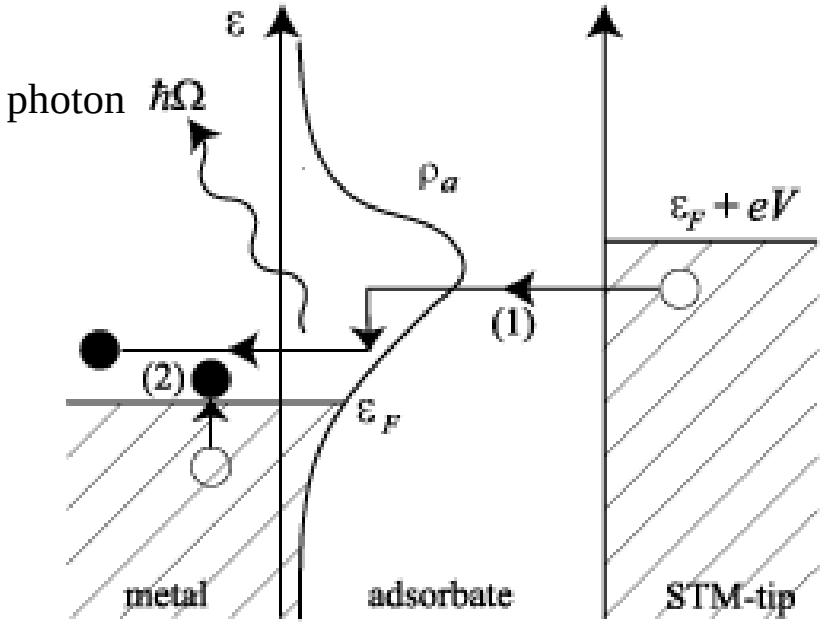

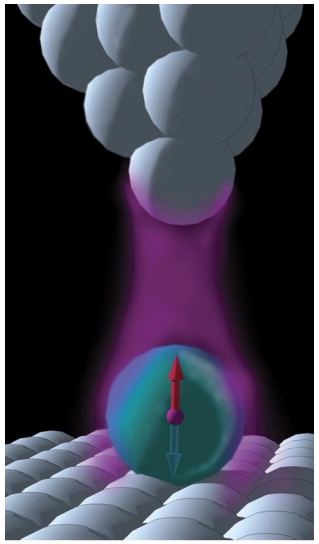

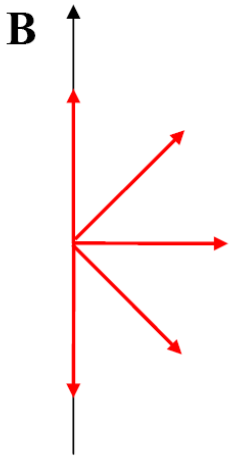

$$\Delta E = \mu_B g_J B \Delta M$$

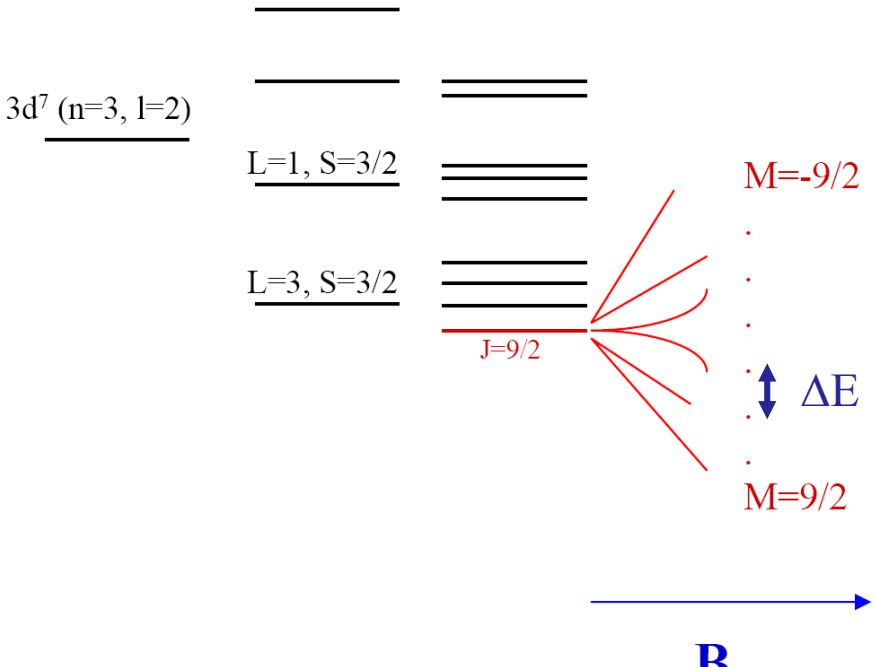

An inelastic tunneling process can also involve energy transfer to excited magnetic states of an atom (spin-flip). The threshold energy for spin-flip processes depends on the environment of magnetic atoms, that is, the coordination of adjacent atoms and their chemical composition, and the magnetic field.

Spin-flip excitation by means of STM

$Mn/Al_2O_3/Ni_3Al(111)$

T = 0.6 K

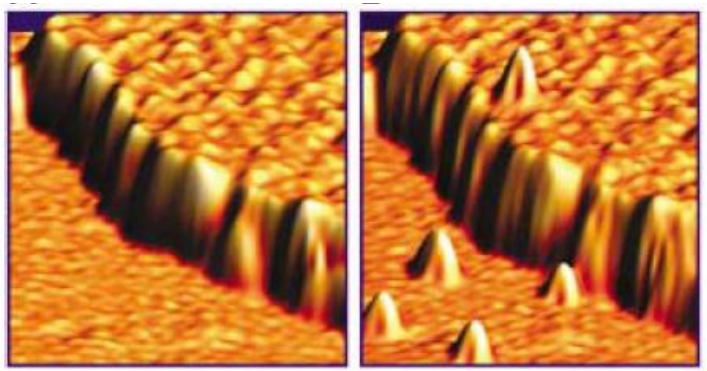

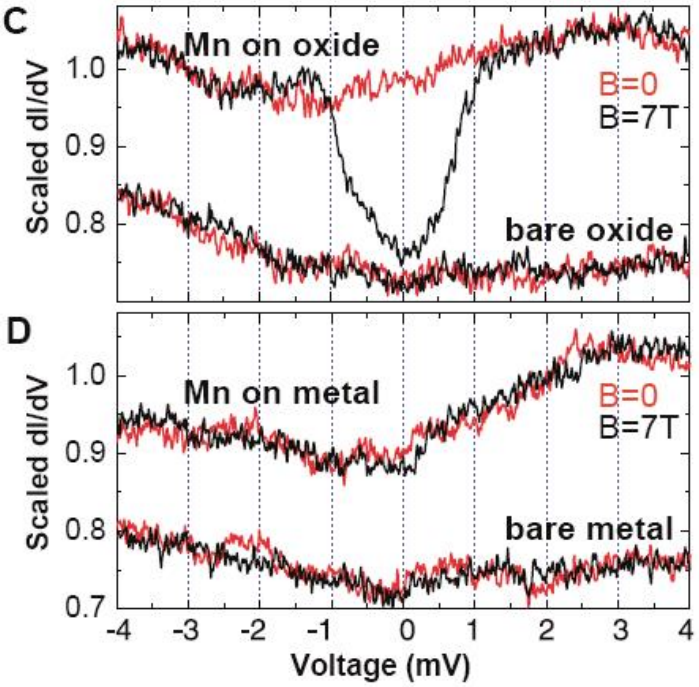

Shift of the spin-flip conductance step with magnetic field

$\Delta E = g_J \mu_B B$

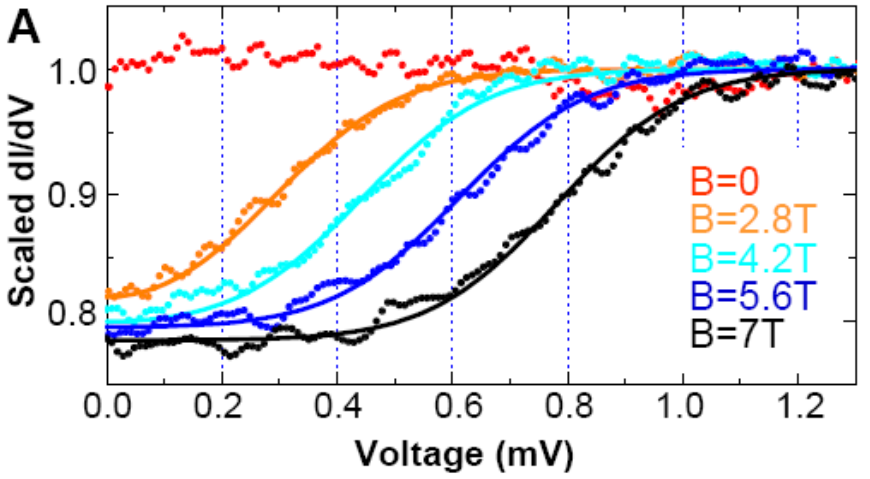

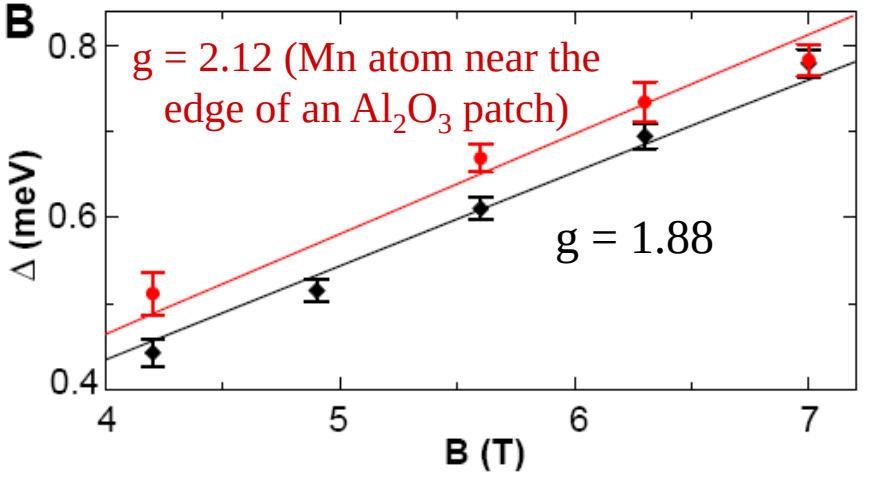

A.J. Heinrich *et al.*, Science **306**, 466 (2004).

Spin-flip excitation by means of STM: Fe/Cu_2N/Cu(001)

Spectra depend on B field direction -> anisotropy

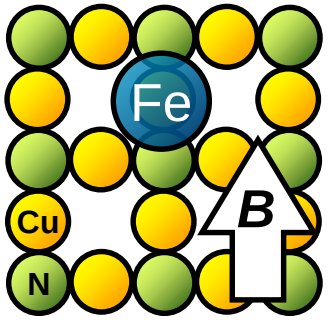

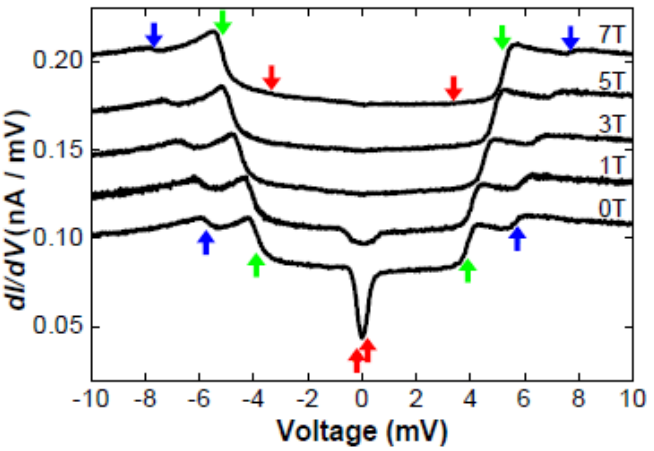

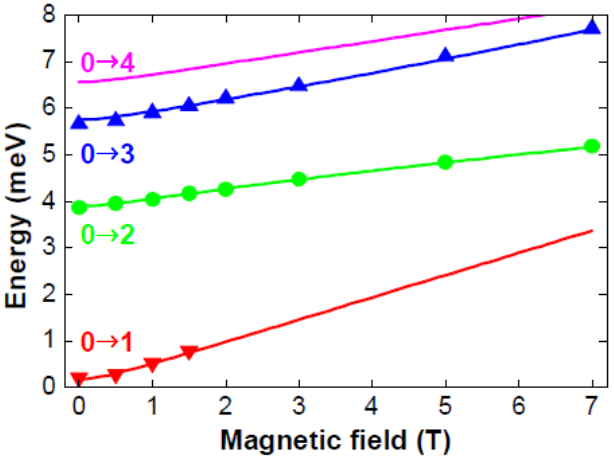

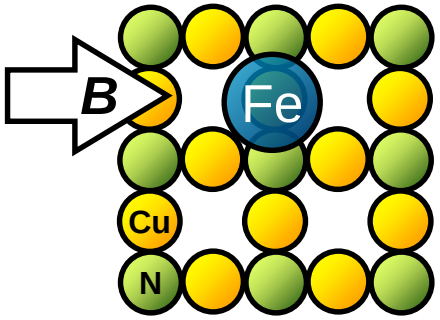

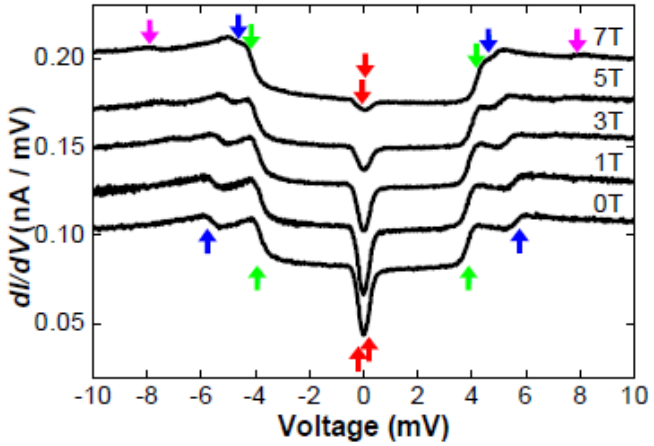

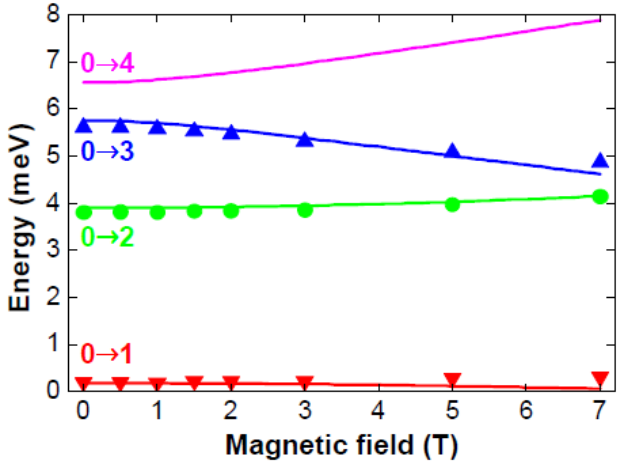

Hirjibehedin *et al.*, Science **317**, 1199 (2007)

Fe/Cu_2N/Cu(001): spin Hamiltonian

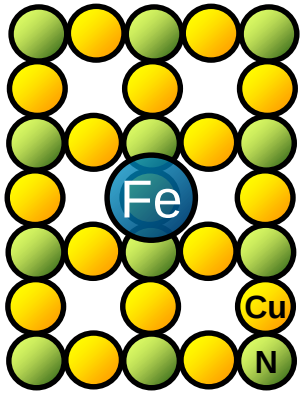

Fe: $3d^6$

$S = 2$

$$H = -g\mu_B \vec{B}\cdot\vec{S} + DS_z^2 + E\left(S_x^2 - S_y^2\right)$$

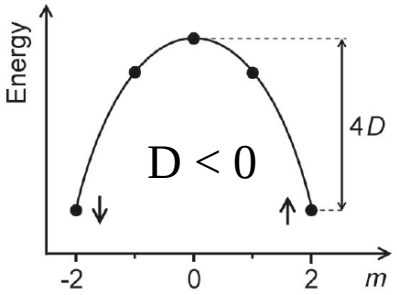

E = 0 -> K = DS^2 (S integer)

K= D (S^2 -1/4) (S half-integer)

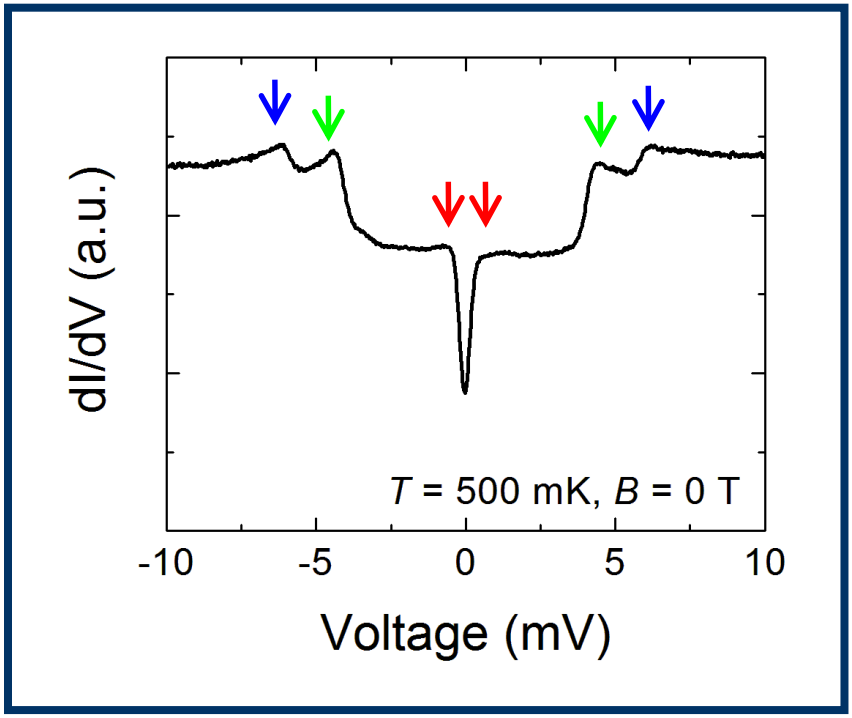

After spin-flip scattering the magnetic atom is excited from its ground state with $S_z = \pm S$ to a state with $S_z = \pm (S - 1)$, i.e., ΔS_z 0, ±1

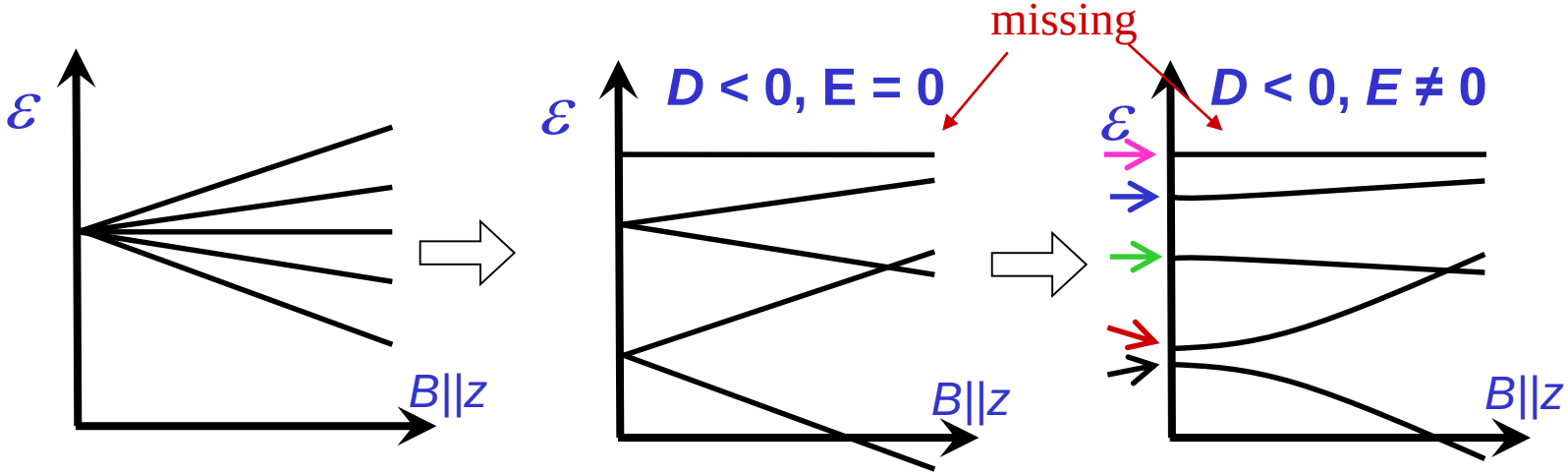

Spin-flip excitation by means of STM: Fe/Cu_2N/Cu(001)

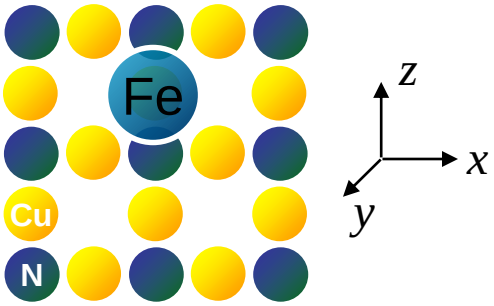

$$H = g\mu_B \vec{B}\cdot\vec{S} + DS_z^2 + E(S_x^2 - S_y^2)$$

$$S = 4\mu_B, D = -1.55\,meV, E = 0.3\,meV$$

Calculate the eigenvectors $|\Psi_i\rangle$ and eigenvalues E_i of H for a given B

Eigenstate	|+2⟩	|+1⟩	|+0⟩	|−1⟩	|−2⟩	Eigenvalues
			$B = 0\ T$			
ψ_0	0.697	0	−0.166	0	0.697	-6.93 meV
ψ_1	0.707	0	0	0	−0.707	-6.74 meV
ψ_2	0	0.707	0	−0.707	0	-3.08 meV
ψ_3	0	0.707	0	0.707	0	-0.58 meV
ψ_4	0.117	0	0.986	0	0.117	0.19 meV
			$B = 7\ T$			
ψ_0	0.021	0	−0.097	0	0.995	
ψ_1	0.987	0	−0.157	0	−0.036	
ψ_2	0	0.402	0	−0.916	0	
ψ_3	0	0.916	0	0.402	0	
ψ_4	0.159	0	0.983	0	0.092	

- S integer, E ≠ 0 -> quantum tunneling: at B = 0 the ground state (ψ_0) has S* = 0
- B splits the states and restore a moment: at B = 7T S* = -2

Spin-flip excitation in atom on metals: Fe on Cu(111)

Conceptually spin-flip excitation should be observed only on atom with localized electrons, but ……

Fe atom

Cu atom

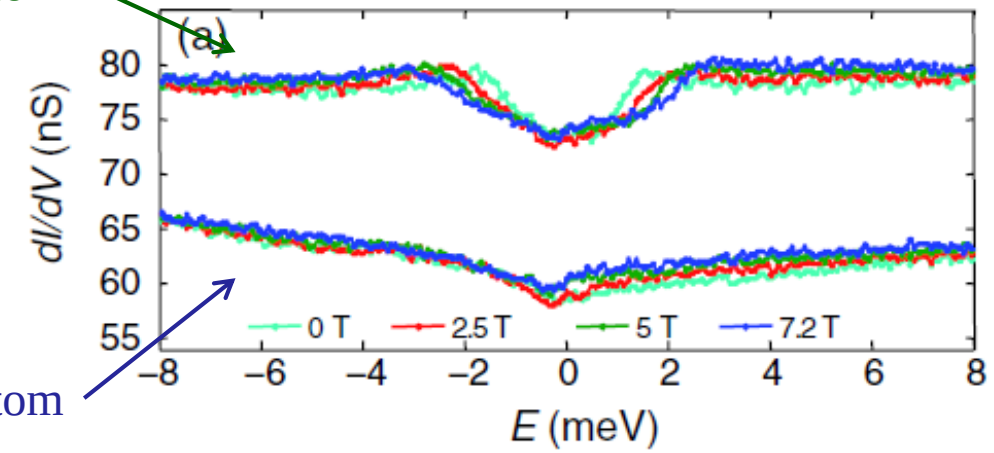

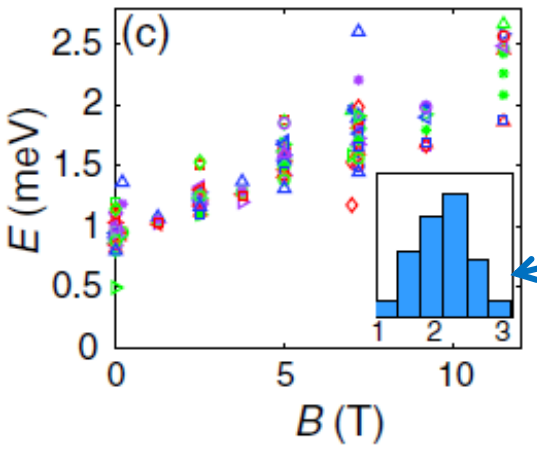

$g_J = 2.1$:
$E = g_J \mu_B B$

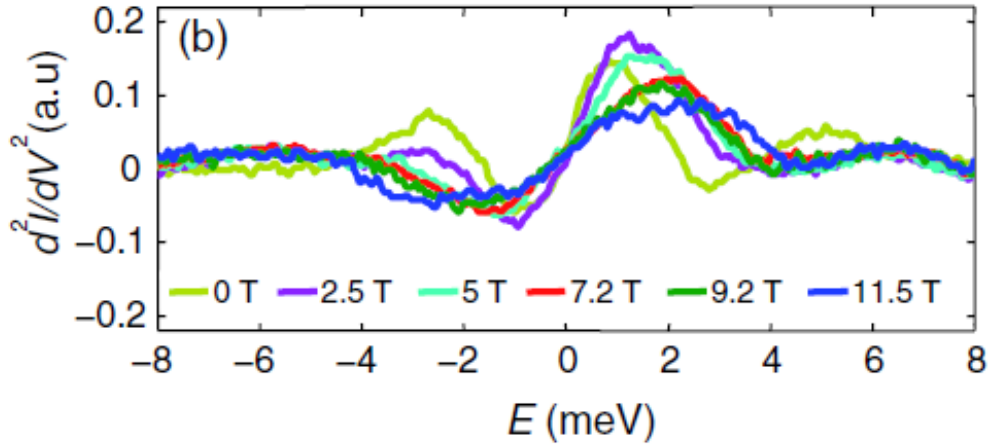

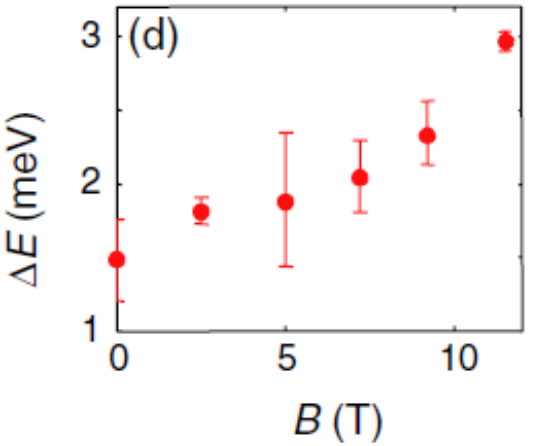

Interaction with the metallic substrate:

- Fe is a d^6 -> L = 2, S = 2, $m_J = 6\ \mu_B$ with $g_J = 1.5$ but experimetally $m_J \sim 3.5\ \mu_B$ with $g_J = 2.1$
- $\tau \sim h/(\Delta E) = 200$ fsec (B = 0 T) -> very short spin-lifetime

A. A. Khajetoorians *et al.*, Phys. Rev. Lett. **106**, 037205 (2011)

Spin-polarized STM

Ferromagnetic (FM) - nonmagnetic (NM) - ferromagnetic (FM) junction

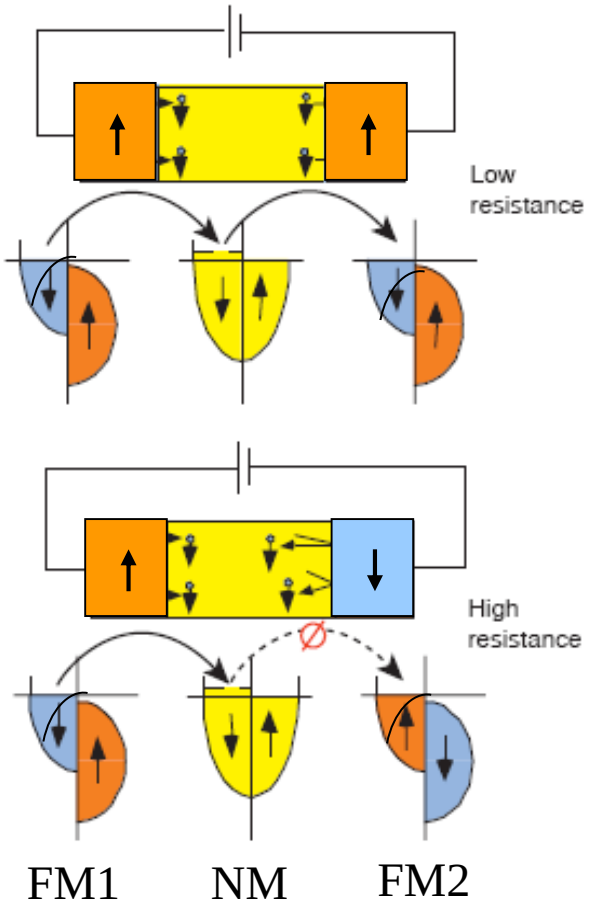

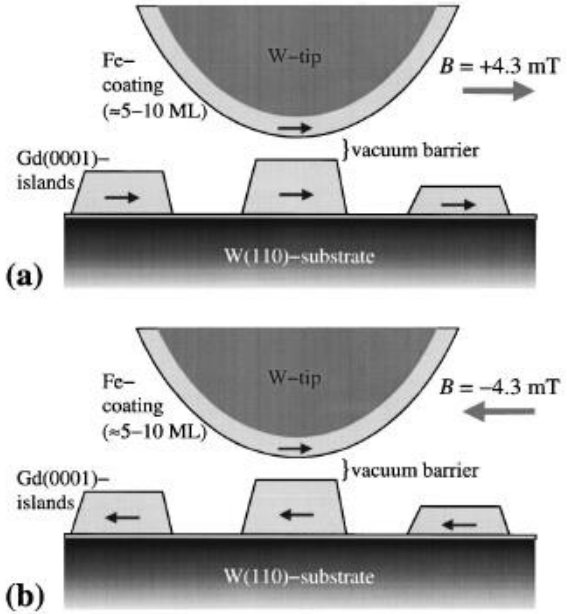

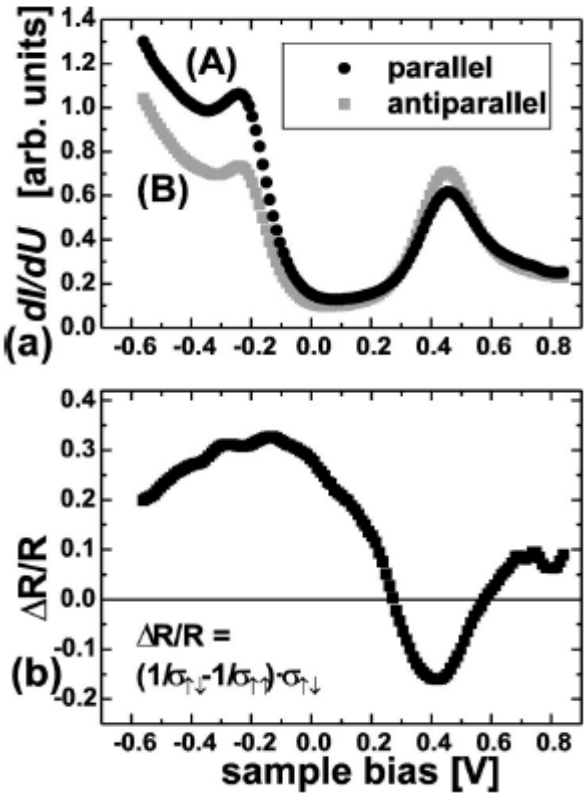

Science **282**, 1660 (1998); R. Wiesenganger, Appl. Phys. Lett. **75,** 124 (1999)

Co/Pt(111): spin polarized STM

F. Meier *et al.*, Science **320**, 82 (2008)

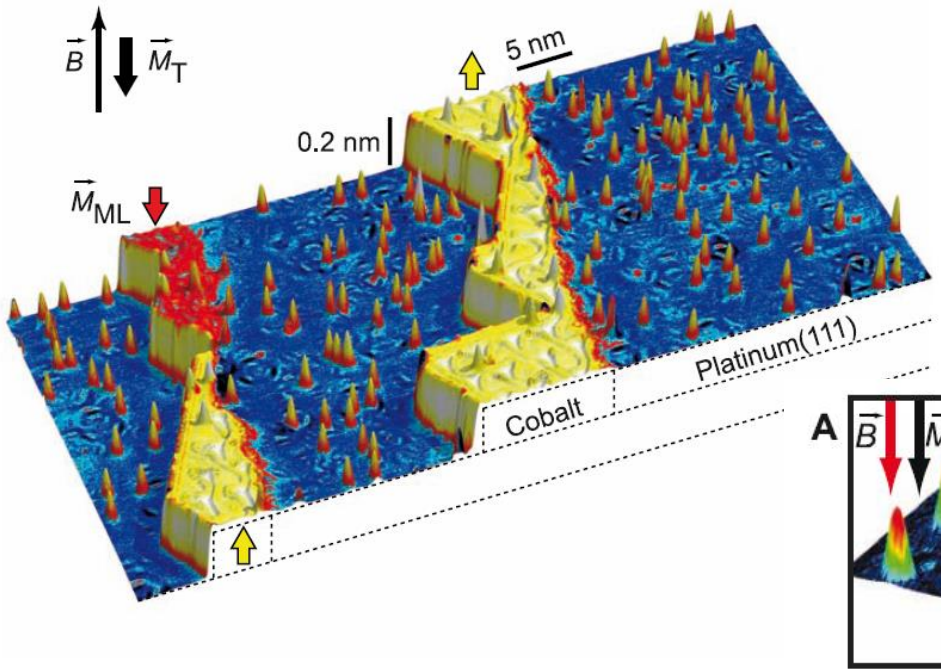

Co adatom on the Pt(111)

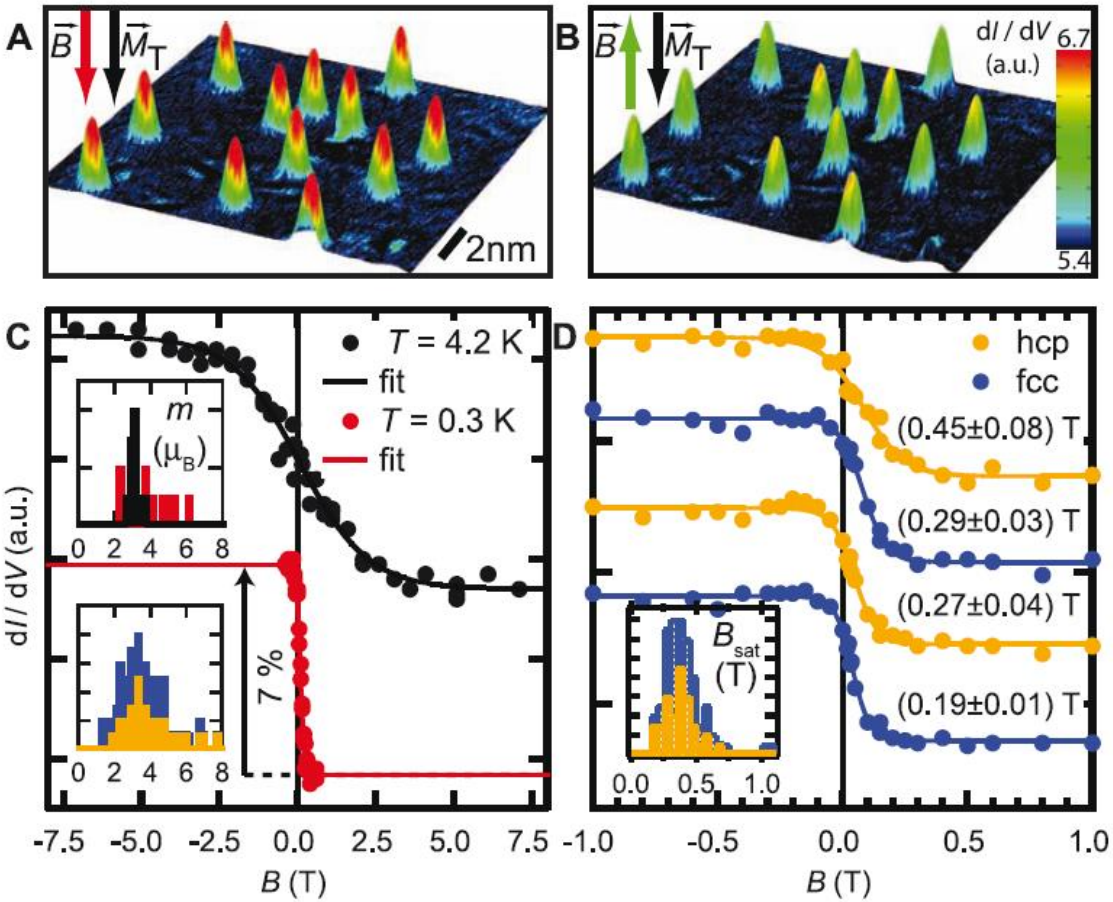

Hysteresis curves on single atoms

K = 9.3 meV

$m_{hcp} = (3.0 \pm 0.3)\mu B$ and

$m_{fcc} = (3.1 \pm 0.1)\mu B$

In agreement XMCD results

No remanence even at T = 0.3 K

N.B.: $\tau = \tau_0 \exp(K/k_B T)$ -> τ ~6 days -> interaction with the substrate electron shortens the spin lifetime

Artificial constructed quantum magnet: read for exercise

A. A. Khajetoorians *et al.*, Science **339**, 55 (2013)

5 Fe atoms cluster on Cu(111)

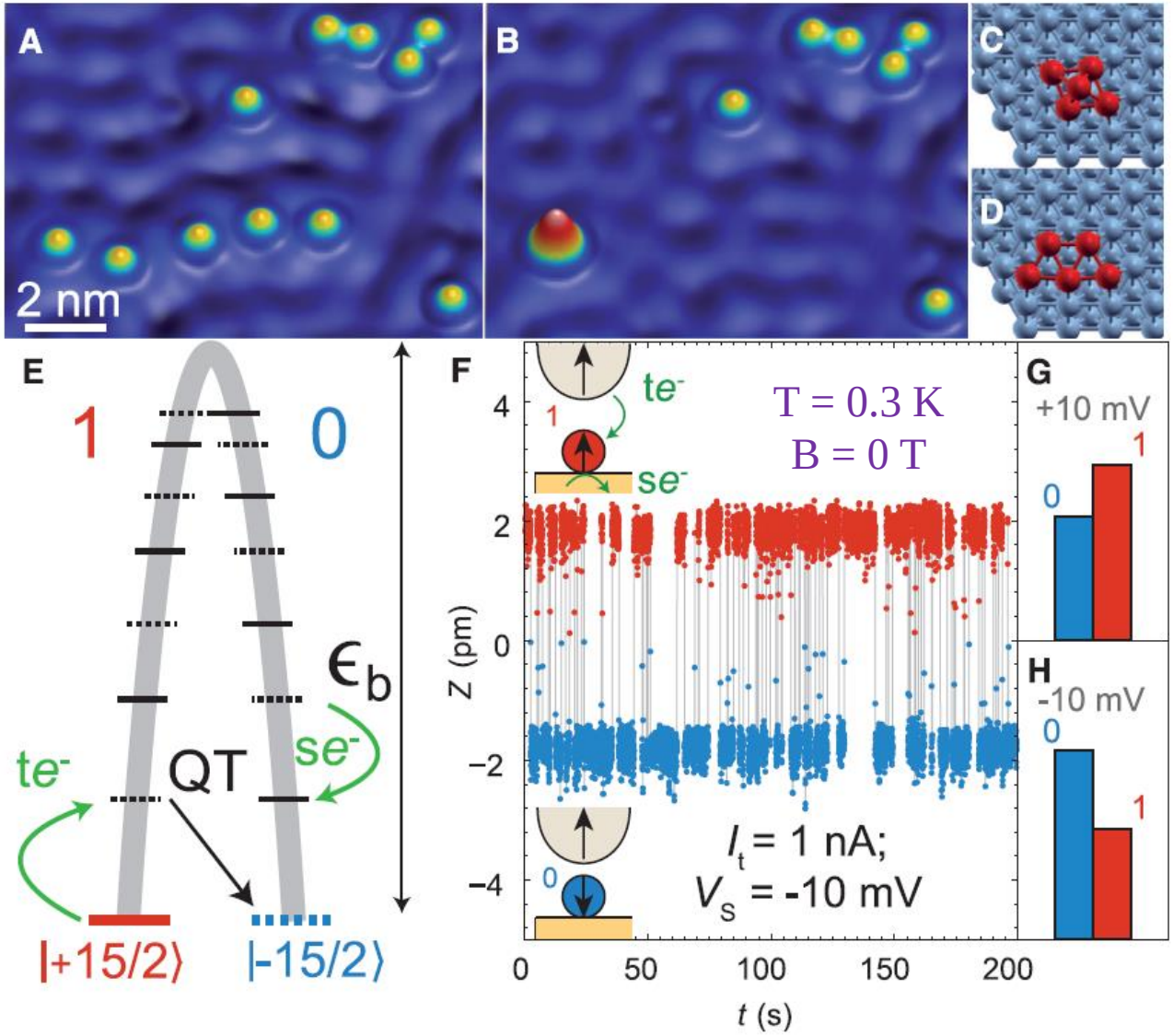

$H = g_J \mu_B H_z J_z + D J_z^2 + E (J_x^2 - J_y^2)$

J = 15/2;
D = -0.1 meV; E = 0.02 meV
$\varepsilon_b = D(J_z^2 - 1/4) = 5.6$ meV

Destabilizing interactions:
- QT (due to E = 0.02 meV)
- spin-flip due to tunneling e⁻ (te⁻)
- spin-flip due to conduction e⁻ (se⁻)

Without destabilizing interactions
$\varepsilon_b = 217$ kT !!!
$\tau = \tau_0 \exp(\varepsilon_b/kT) \sim 10^{84}$ s !!!

Artificial constructed quantum magnet

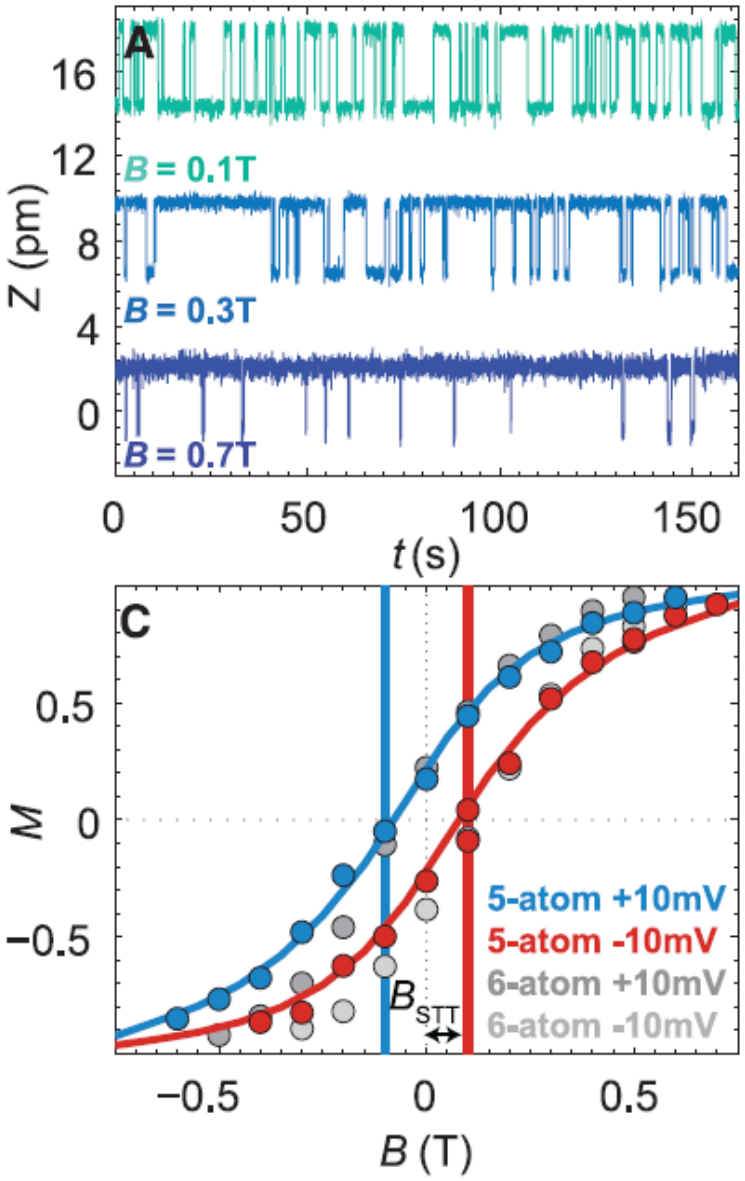

The magnetic field stabilizes one of the two ground states

Remanence observed at T = 0.3K

A. A. Khajetoorians *et al.*, Science **339**, 55 (2013)

Antiferromagnetic bits

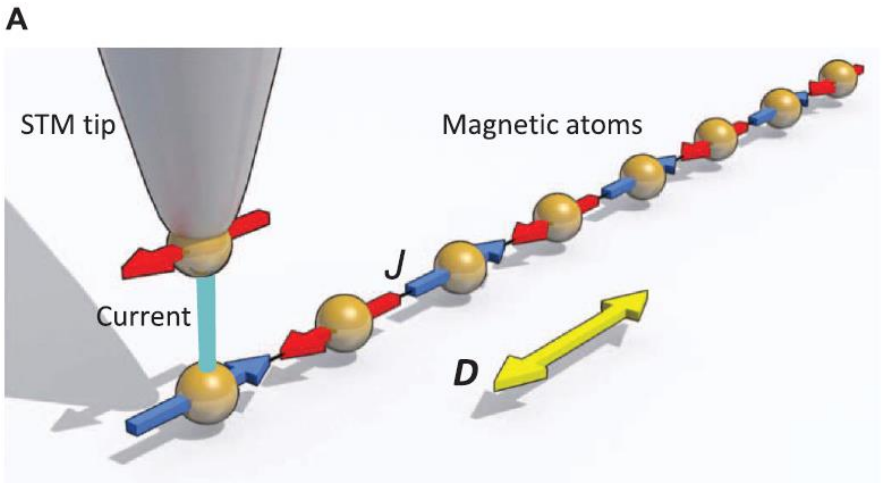

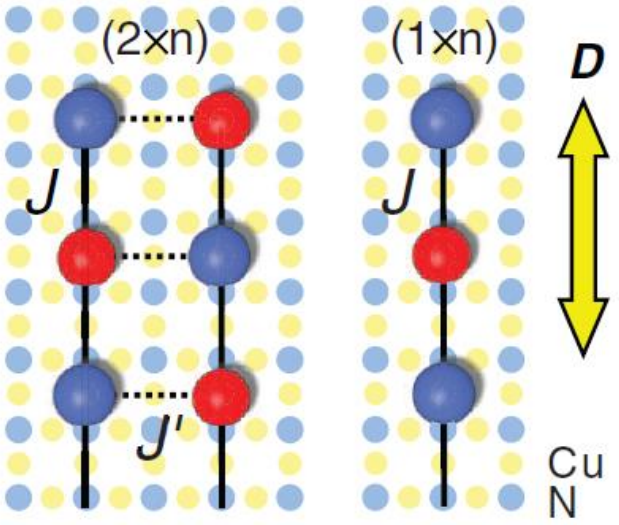

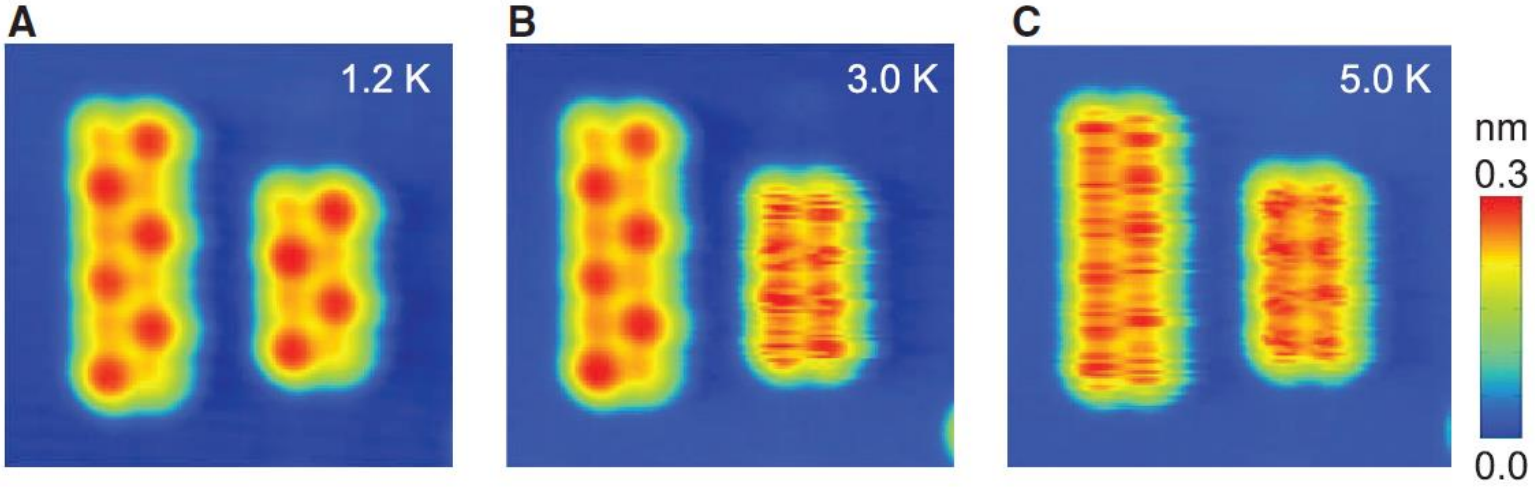

S. Loth *et al.*, Science **335**, 196 (2012)

Antiferromagnetic bits

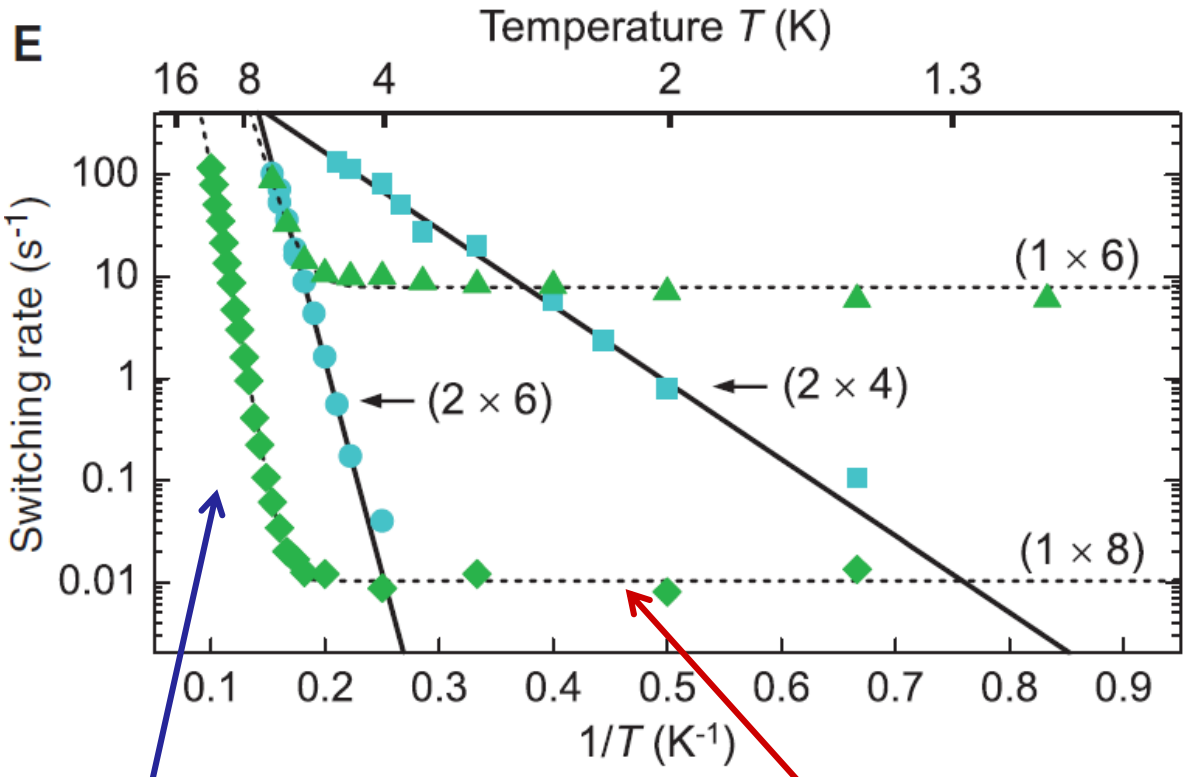

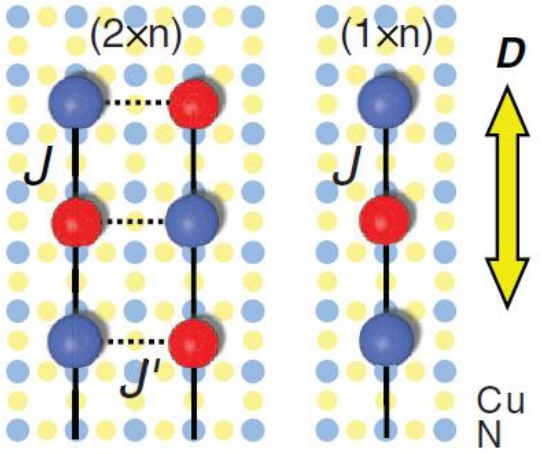

Arrhenius behavior:
Reversal over a barrier

Temperature independent:
Quantum tunneling

Experimentally, quantum tunneling is reduced by:
a) increasing the length or
b) by exchange coupling two lines

S. Loth *et al.*, Science **335**, 196 (2012)

Antiferromagnetic bits

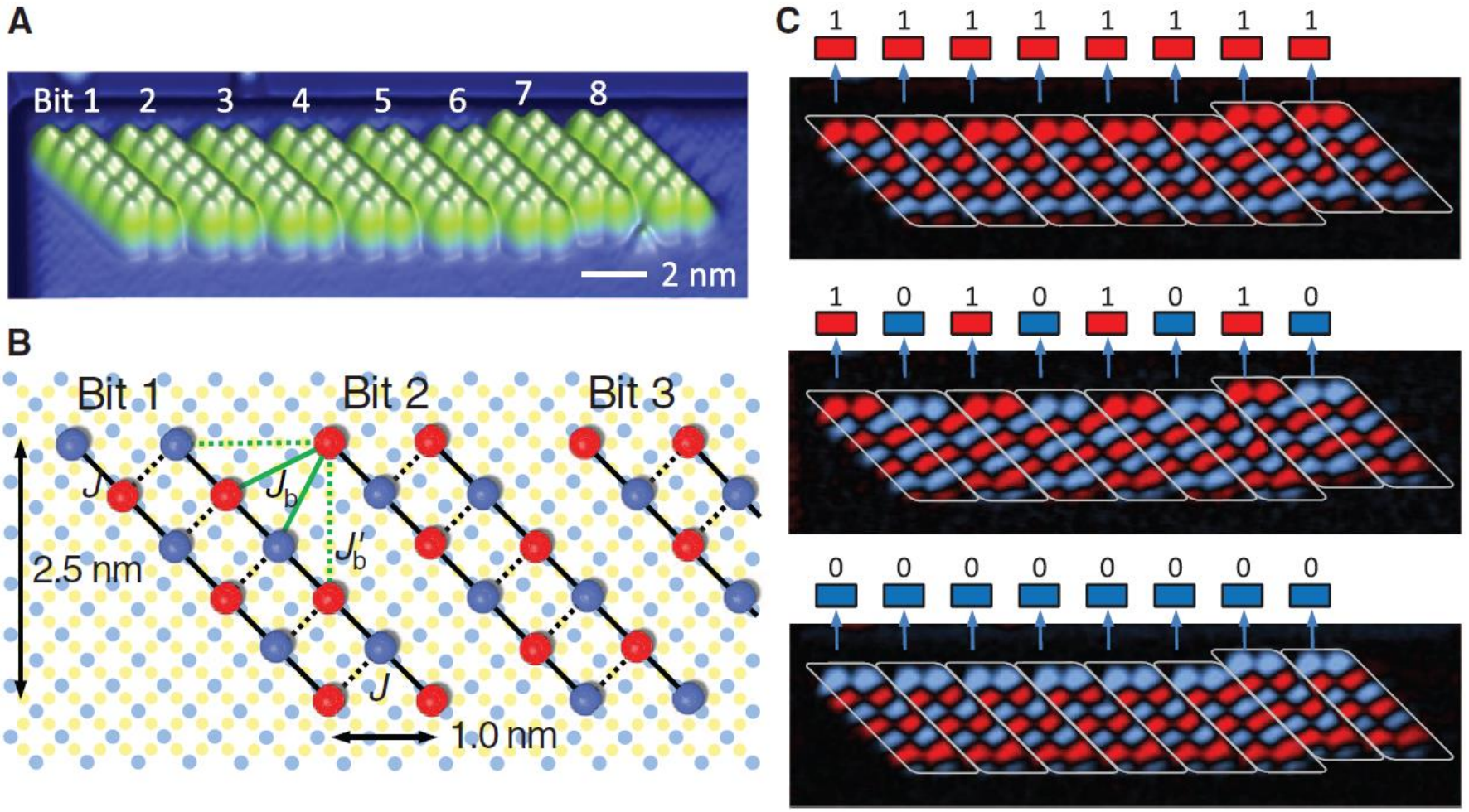

S. Loth *et al.*, Science **335**, 196 (2012)

Spin-resolved DOS in nano-islands: Co/Cu(111)

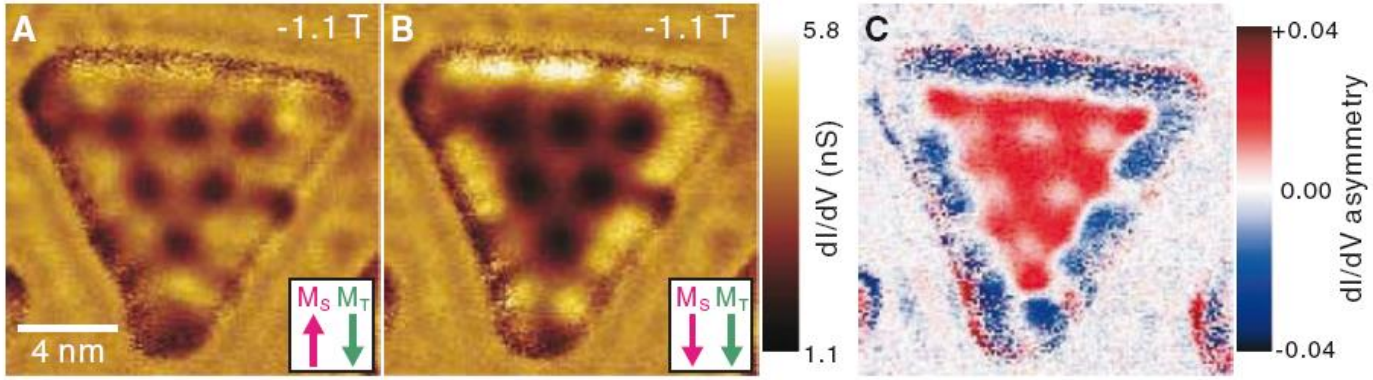

Fig. 2. (**A** and **B**) Two *dI/dV* images of the Co island in Fig. 1, the basis for the *dI/dV* asymmetry map in (C). Both images were recorded at $B = -1.1$ T, but with different magnetization configurations between the magnetic tunneling tip and the Co island: antiparallel (A) and parallel (B). The insets represent the antiparallel (AP) and parallel (P) configurations. $V = +0.03$ V, $V_{stab} = +0.5$ V, and $I = 1.0$ nA, where V is the bias voltage at which the *dI/dV* signal is recorded and V_{stab} is the bias voltage to stabilize the tip before the feedback loop is opened (*10*). (**C**) *dI/dV* asymmetry map calculated using Eq. 1 from the images in (A) and (B).

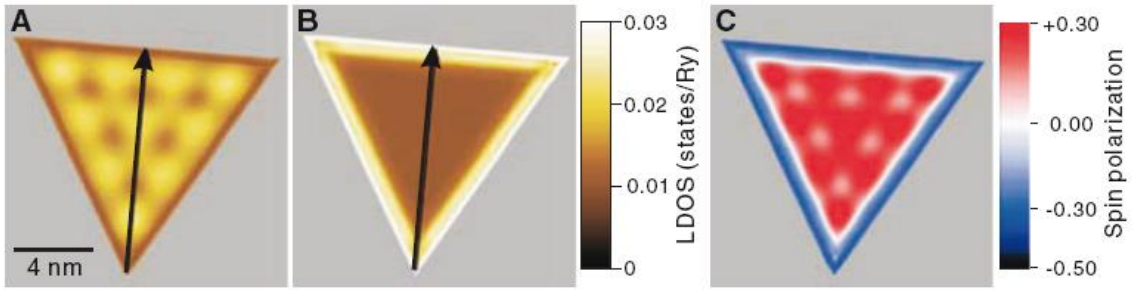

Spatially modulated spin-resolved DOS

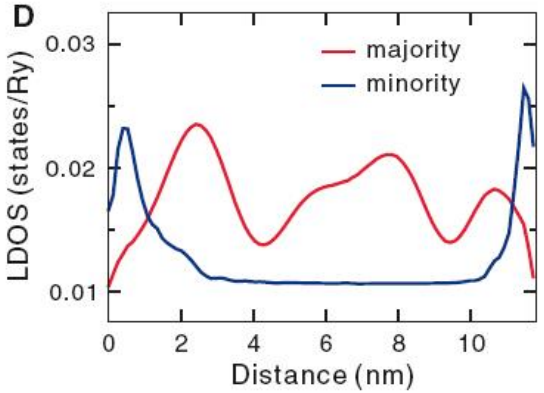

Fig. 3. Calculated spin polarization map of a triangular two-atomic-layer Co island on Cu(111). (**A** and **B**) LDOS maps for the majority (A) and the minority (B) state electrons at the Fermi level. (**C**) Spin polarization map calculated from the two LDOS maps in (A) and (B) from Eq. 3. (**D**) Line scans along the black arrows in (A) and (B).

H. Oka *et al.*, Science **327**, 843 (2010); O. Pietzsch *et al.*, Phys. Rev. Lett. **96**, 237203 (2006)

Spin-resolved DOS in nano-islands: Co/Cu(111)

The dominant spin character depends on the energy

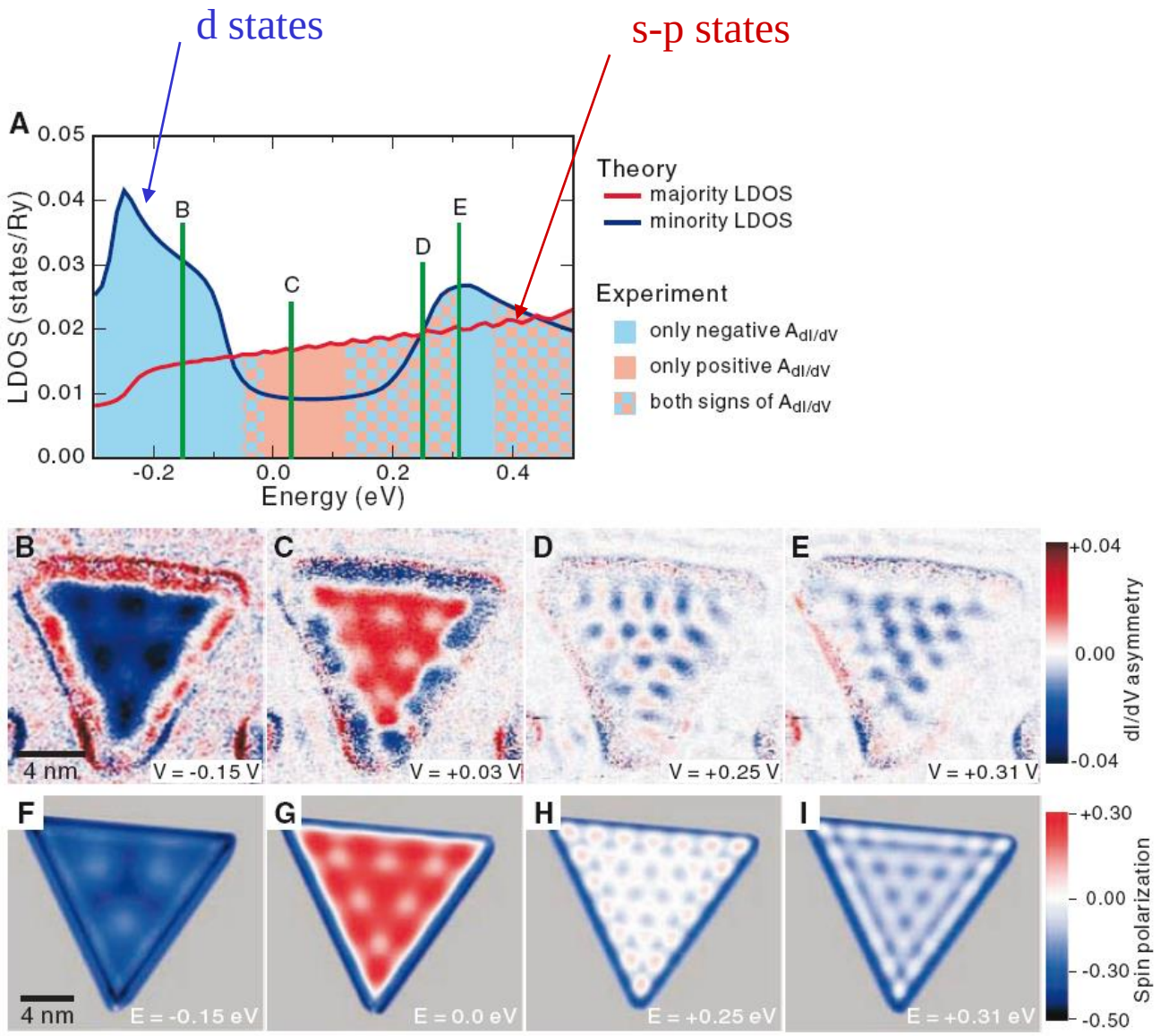

Fig. 4. Energy dependences of the measured *dI/dV* asymmetry maps and calculated spin polarization maps of the Co islands. (**A**) Calculated spin-resolved LDOS of a two-atomic-layer Co film on Cu(111). (**B** to **E**) Experimental *dI/dV* asymmetry maps measured on the Co island of Fig. 1. The *dI/dV* asymmetry maps are calculated from two *dI/dV* images measured at AP and P states from Eq. 1. Measurement conditions of *dI/dV* images: $B = -1.1$ T, $V_{stab} = +0.5$ V, $I = 1.0$ nA. (**F** to **I**) Calculated spin polarization maps of the triangular Co island. The spatial dependence of the spin polarization as defined by Eq. 3 is shown by the maps, which are calculated from two LDOS maps for the majority and the minority states. Vertical green lines in (A) correspond to the energy positions where the *dI/dV* asymmetry maps are obtained. A color map in (A) indicates the energy area where experimental results for the inner part of the Co island show only positive (blue), only negative (red), or both signs (lattice pattern with blue and red) of the *dI/dV* asymmetry in the *dI/dV* asymmetry maps.

H. Oka *et al.*, Science **327**, 843 (2010)